REVIEW

Review of organic and inorganic pollutants removal by biochar and biochar-based composites

Liping Liang[1] · Fenfen Xi[1] · Weishou Tan[1] · Xu Meng[2] · Baowei Hu[1] · Xiangke Wang[1]

Abstract

Biochar (BC) has exhibited a great potential to remove water contaminants due to its wide availability of raw materials, high surface area, developed pore structure, and low cost. However, the application of BC for water remediation has many limitations. Driven by the intense desire of overcoming unfavorable factors, a growing number of researchers have carried out to produce BC-based composite materials, which not only improved the physicochemical properties of BC, but also obtained a new composite material which combined the advantages of BC and other materials. This article reviewed previous researches on BC and BC-based composite materials, and discussed in terms of the preparation methods, the physicochemical properties, the performance of contaminant removal, and underlying adsorption mechanisms. Then the recent research progress in the removal of inorganic and organic contaminants by BC and BC-based materials was also systematically reviewed. Although BC-based composite materials have shown high performance in inorganic or organic pollutants removal, the potential risks (such as stability and biological toxicity) still need to be noticed and further study. At the end of this review, future prospects for the synthesis and application of BC and BC-based materials were proposed. This review will help the new researchers systematically understand the research progress of BC and BC-based composite materials in environmental remediation.

Keywords Biochar magnetic composites · Nanometallic oxide/hydroxide biochar composites · Biochar based 2D membrane · 3D biochar-based macrostructures · Biological toxicity

1 Introduction

Along with the rapid growth of industry and economy, water pollution has seriously endangered the environment and human health. Most of the pollutants in aqueous solutions come from chemical pollution, including heavy metals (Cu, Cr, Pb, Ni, etc.) (Islam et al. 2015), metalloids (Se, As, etc.) (Bender et al. 1995) and organic pollutants (dyes, antibiotics, etc.) (Hao et al. 2021; Schwarzenbach et al. 2010; Yao et al. 2020). Heavy metals are not biodegradable and tend to accumulate in living organisms through the food chain. Organic pollutants, because of high persistence, difficult

removal, easy transfer, and extreme toxicity pose a serious threat to human health (Houde et al. 2008; Liu et al. 2021a, b). Facing severe water pollution, there is urgent need to find cost-effective technologies based on low-cost materials. Among numerous separation technologies for contaminants in wastewater treatment, adsorption is preferred owing to its relatively high efficiency, low cost, and easy operation (Huggins et al. 2016). Recenrly, BC has become a new sorbent for its superior properties, such as eco-friendliness, abundant in functional groups and inorganic mineral species, containing micro and/or meso-porous structures and high adsorption capacity, which were widely employed to remove the contaminants from wastewater (Shaheen et al. 2019; Hu et al. 2020). Moreover, BC's feedstocks are stem from solid waste, agricultural biomass, animal litters, and the preparation does not need activation, which means BC has a great potential in environmental remediation (Liu and Zhang 2011). Nonetheless, there are still some limitations of the pristine BC to selectively adsorb high concentration contaminants (Ma et al. 2014). To overcome this shortage, the BC-based composite materials were obtained by further

✉ Baowei Hu
hbw@usx.edu.cn

✉ Xiangke Wang
xkwang@ncepu.edu.cn

1 College of Life Science, Shaoxing University, Shaoxing 312000, People's Republic of China

2 College of Textile and Garment, Shaoxing University, Shaoxing 312000, People's Republic of China

activation and modification to improve the specific surface area, pore structure, and surface functional groups (Zhang et al. 2015; Xue et al. 2012). BC-based composite materials can be selectively designed or produced for the target pollutants by adding functional materials, magnetic substances, and nanoparticles. Those composite materials are rich in functional groups that can make up the shortage of pristine BCs in environmental remediation.

As is known to all, the contaminant's removal efficiency and mechanisms of BC and BC-based composite materials were related to the mineral content, ionic content, organic functional groups, etc. (Shaheen et al. 2019). However, the performances of BC and BC-based composite materials were also related to biomass, reaction parameters, etc. For example, the pH value of BC prepared at a higher temperature was relatively high, while BC prepared under lower temperature contained more toxic substances, such as polycyclic aromatic hydrocarbons (PAH), polychlorinated dibenzo dioxins (PCDD), and polychlorinated dibenzo furans (PCDF). And BC stemming from animal manure was rich in ash. Currently, a variety of studies confirmed that BC-based composites could significantly improve the performance of contaminants removal. For instance, Ioannou et al. (2019) reported that 100% U(VI) from aqueous solutions could be removed by MnO_2-BC and the maximum adsorption capacity (q_m) reached 904 mg/g. Similarly, Khataee et al. (2017) synthesized TiO_2-BC, which enhanced the sonocatalytic degradation efficiency of Reactive Blue 69 (RB69) from 63.8 to 98.1%, and the removal efficiency was still 92.1% after five successive processes in this systems. So, it was necessary to develop some new strategies for new BC-based materials such as 2D membranes, 3D carbonaceous hydrogels/aerogels or immobilized microorganisms on it to better remove contaminants.

However, applications of BC particles and BC-based composites inevitably release fine particles into the environment which may cause biological toxicity and damage human health (Lu et al. 2020; Lian and XIng 2017; Zhang et al. 2019b). For example, the addition of rice straw BC into contaminated soil reduced the bioavailability of Pb; meanwhile, DOC, PO_4^{2-} Cl^-, and SO_4^{2-} were released. Other researchers found that under oxidizing conditions, the application of BC in soil remediation increased the concentration of As and Co in the dissolved phase. All of these toxic chemicals may transfer into food chains and cause toxic or side effects on human and environmental health (El-Naggar et al. 2019b, c; Rinklebe et al. 2020). Besides, BC-treated soil may change the pH value, which will have an impact on organisms (El-Naggar et al. 2018; Kookana et al. 2011).

In this paper, we summarized the physicochemical properties of biochar, the preparation method, the performance, and the mechanisms of BC, and BC-based composite materials for contaminants removal, and reviewed the latest progress of BC-based materials in the removal of inorganic and organic pollutants from water and soil. Finally, the potential risks of BC applications and future directions are briefly described.

2 The physicochemical properties of biochar

BC is a carbon-rich solid product obtained by pyrolysis of biomass under oxygen-limited or anaerobic environments (Yi et al. 2017). Because of the large specific surface area, rich porous structure, abundant surface functional groups, and high mineral content, BC has been applied in various fields including energy production, water contaminants treatment, and other fields (Tan et al. 2015). Meanwhile, BC is produced from various biomasses, such as straw (Qiu et al. 2009), corn cob (Mullen et al. 2010), animal manure (Zhang et al. 2013), and wastewater sludges (Lu et al. 2011) (Table 1 for details). BC derived from plant biomass with lignin and cellulose could form porous structures which were beneficial to removing contaminants by pore-filling effect (Kumar et al. 2011). In addition, the plant biomass has a large content of carbon and oxygen elements which can produce various functional groups (–COOH, –C–O–R, -C–OH) on the surface of BC; these groups can serve as additional active sites to improve the removal efficiency (Takaya et al. 2016). BC made from animal manure (pig manure, chicken manure, cow manure) has higher ash content (60% higher than the average, up to 96%) which can be ascribed to the high content of minerals in biomass (such as quartzite, calcite) (Shinogi and Kanri 2003; Cao and Harris 2010). Recent studies showed that the pH of BC from animal manure pyrolysis is higher than that from plants (Shinogi and Kanri 2003).

To our current knowledge, biomass and carbonization process play key roles in BC physicochemical properties. Carbonization processes mainly included pyrolysis, hydrothermal carbonization (HTC), and gasification, which can affect yields, ash content, specific surface area, pH value, surface functional groups, and pore size of BC (Yang et al. 2019).

Pyrolysis is a common decomposition for biomass under anaerobic conditions in the temperature range of 300–900 °C. The biomass and parameters (pyrolysis temperature, heating rate, and residence time) can affect the products during the pyrolysis processes (Ronsse et al. 2013), as shown in Table 2. Generally, higher pyrolysis temperature decreased the BC yield due to larger primary decomposition or secondary decomposition of carbon residual (Angin 2013). Furthermore, Al-wabel et al. (2013) reported that the ash content, specific surface area, and pH value increased with the increase of pyrolysis temperature, while H/C (higher aromaticity) and (O + N)/C (lower polarity) decreased. The increase of pH may be owing to

Table 1 The preparation method of biochar from biomass

Material	Pyrolysis temperature (°C)	Residence time (h)	Heating rate (°C / min)	Pyrolysis mode	Target pollutant	References
Rice straw and swine manure	300	4.0	15	Slow pyrolysis	Cd^{2+}	Deng et al. (2018)
Municipal sewage	450	0.5	10	Slow pyrolysis	Triclosan	Wang and Wang (2019)
Artemisia argyi stem	300–600	–	–	–	Cr(VI) and Cu(II)	Song et al. (2019)
Corn stover	200–300	–	10	Slow pyrolysis	U(VI)	Li et al. (2019a)
Pig manure	300–700	4.0	15	Slow pyrolysis	Cd^{2+}	Zhang et al. (2013)
Orange peel	150–700	–	–	Slow pyrolysis	Naphthalene and 1–naphthol	Chen and Chen (2009)
Rice husk	600	4.0	20	–	As(III), As(V) and Cd(II)	Wang et al. (2019a)
Pineal shell	350–550	–	–	Slow pyrolysis	Phenol	Mohammed et al. (2018)
Oak	400, 450	–	–	Fast pyrolysis	Cd^{2+} and Pb^{2+}	Mohan et al. (2013)
Sludge	550	2.0	10	Slow pyrolysis	Pb^{2+}	Lu et al. (2011)
Cow dung	200, 350	4.0	–	Slow pyrolysis	Pb^{2+} and atrazine	Cao et al. (2008)
Algae	203	2.0	–	HTC	–	Heilmann et al. (2010)
Municipal sludge	500–900	–	–	Fast pyrolysis	Cd^{2+}	Chen et al. (2014)
Cottonseed hull	200–800	4.0	–	Slow pyrolysis	Ni^{2+}, Cu^{2+}, Pb^{2+}, Cd^{2+}	Uchimiya et al. (2011)

Table 2 Effects of pyrolysis temperature on the biochar physicochemical properties

Raw material	T (°C)	Yield (%)	Ash (%)	BET (m²/g)	V_{total} (cm³/g)	pH	H/C	O/C	References
Pineal shell	350	36.53	2.46	0.82	0.001	7.1	0.06	0.32	Mohammed et al. (2018)
	450	33.09	2.75	1.29	0.005	7.8	0.05	0.27	
	550	29.23	3.23	228.11	0.038	8.7	0.04	0.15	
Alfalfa	350	47.70	7.10	3.50	–	–	0.80	0.20	Choi and Kan (2019)
	450	30.70	9.10	4.00	–	–	0.50	0.10	
	550	28.30	16.0	183.00	–	–	0.30	0.10	
	650	27.50	13.6	405.00	–	–	0.20	0.10	
Rice straw	300	38.00	–	6.77	–	7.9	0.07	0.43	Shen et al. (2019)
	500	31.00	–	22.38	–	10.4	0.04	0.22	
	700	30.00	–	115.47	–	10.7	0.03	0.13	
Oange peel	200	61.60	0.30	7.75	0.010	–	1.14	0.45	Chen and Chen (2009)
	300	37.20	1.57	32.30	0.031	–	0.78		
	400	30.00	2.10	34.00	0.010	–	0.58	0.22	
	500	26.90	4.27	42.40	0.020	–	0.38	0.21	
Soybean stover	300	37.03	10.41	5.61	–	7.3	0.74	0.27	Ahmad et al. (2012)
	700	21.59	17.18	420.30	0.190	11.3	0.19	0.14	
Peanut shell	300	36.91	1.24	3.14	–	7.8	0.67	0.29	
	700	21.89	8.91	448.20	0.200	10.6	0.25	0.12	
Municipal sewage sludge	500	63.10	74.21	25.42	0.056	8.8	0.09	0.45	Chen et al. (2014)
	600	60.25	77.90	20.27	0.053	9.5	0.06	0.30	
	700	58.66	81.53	32.17	0.068	11.1	0.04	0.30	
	800	54.71	83.93	48.50	0.090	12.2	0.04	0.17	
	900	53.31	88.07	67.60	0.099	12.2	0.08	0.12	
Rice straw	300	36.90	13.40	20.20	–	8.2	0.07	0.36	Fan et al. (2018)
	500	30.10	28.40	50.11	–	9.7	0.04	0.27	
	700	16.80	34.20	288.34	–	10.0	0.03	0.25	

the volatilization during pyrolysis and releasing of alkali salt during pyrolysis (Lehmann et al. 2011). The increase of ash contents and specific surface area was attributed to the loss of carbon components at the high temperature and the increasing micropore volume (Park et al. 2015). Moreover, higher pyrolysis temperature can remove labile materials, form a larger number of relatively small pores, and increase the total pore volume of BC (Zhao et al. 2018; Lee et al. 2010). However, Lyu et al. (2016) revealed that BC prepared at lower temperatures produced aryl hydrocarbon receptor (AhR) which was toxic to microorganisms by inducing AhR mediated effects.

According to the heating rate, pyrolysis processes were divided into slow pyrolysis and fast pyrolysis (Cha et al. 2016). Different heating rates showed effects on BC yields at the low temperature, but could be ignored at the high temperature. For instance, Angin (2013) pyrolyzed the safflower seed press cake with different heating rates at 400 °C, and the yield decreased from 34.18 to 29.70% with the increase of heating rate. At a pyrolysis temperature of 600 °C, the yield changed only 1.76%. However, Zhao et al. (2018) reported that the effect of the heating rate had no obvious relationship with BC yields. The study of Angin (2013) showed that the specific surface area decreased with the increase of the heating rate. However, Zhao et al. (2018),

Li et al. (2016), and Mohanty et al. (2013) suggested that the specific surface area increased significantly with the increase of the heating rate. Zhao et al. (2018) showed that as the heating rate increased from 1 to 20 °C/min, the surface area was increased about 30%. This may be attributed to the faster heating rate and can lead to a larger extent of thermal decomposition. However, a lower heating rate may be benefit to the stability of BC and generated more aromatic structures than the higher heating rate (Leng and Huang 2018; Pereira et al. 2011). But, when the heating rate was in the range of 5–20 °C, other properties (such as pore volume, H/C, O/C ratio, and fixed carbon) were little affected (Cross and Sohi 2013). The effects of heating rate on biochar physicochemical properties were summarized in Table 3.

To our current knowledge, residence time can affect the yields and properties of BC. Recently, Wang et al. (2019b) demonstrated that the yield significantly decreased with the increase of residence time. In addition, the production of tar and biogas both increased, which was ascribed to the pyrolysis of volatile substances in biomass. However, Sun et al. (2016) suggested that the residence time showed little effect on the yields at a high temperature, which is consistent with Leng and Huang (2018) and Zhao et al. (2018). High temperature mainly affected the specific surface area and internal structure of BC, but had little

Table 3 Effects of heating rate on the biochar physicochemical properties

Biomass	T (°C)	Heating rate (°C / min)	Yield (%)	Ash (%)	BET (m²/g)	V_{Total} (cm³/g)	pH	H/C	O/C	References
Safflower seed press cake	400	10	34.18	7.50	2.67	0.005	8.2	0.71	0.26	Angin (2013)
		30	30.00	8.40	2.26	0.004	7.6	0.6	0.27	
		50	29.70	8.50	1.89	0.004	8.1	0.64	0.26	
	500	10	28.90	8.50	4.23	0.080	9.4	0.5	0.23	
		30	27.80	8.60	3.98	0.075	9.5	0.49	0.25	
		50	26.00	8.70	3.64	0.069	9.3	0.48	0.23	
	600	10	26.20	9.20	3.41	0.006	9.9	0.38	0.2	
		30	25.30	9.30	2.85	0.005	10.2	0.38	0.21	
		50	24.40	9.50	2.47	0.005	9.8	0.43	0.21	
Rapeseed stem	650	1	–	9.79	295.90	0.166	–	0.21	0.07	Zhao et al. (2018)
		10		8.64	316.90	0.180		0.22	0.07	
		20		9.80	384.10	0.219		0.23	0.07	
Pinewood sawdust	500	5	27.46	2.68	–	–	–	0.44	0.11	Li et al. (2016)
		10	26.59	2.89	191.80			0.46	0.08	
		15	24.80	3.62	–			0.44	0.09	
Wheat straw	450	2	–	3.90	178.00	0.184	–	0.40	0.40	Mohanty et al. (2013)
		450		3.60	184.00	0.179		0.60	0.40	
Timothy grass		2		3.50	179.00	0.188		0.40	0.30	
		450		3.10	203.00	0.198		0.70	0.40	
Pinewood		2		4.60	166.00	0.167		0.40	0.10	
		450		4.10	185.00	0.178		0.60	0.20	

effect on the yields (Braadbaart and Poole 2008). Zhao et al. (2018) claimed that the surface area and morphology were significantly influenced by residence time. The specific surface area increased with the increase of residence time, then decreased slightly, which may be owing to the fact that a longer residence time destroyed the cell structure, then affected the surface morphology of BC. Furthermore, Tan et al. (2017) showed that as the residence time increased, the pore size of BC increased and then decreased. When the residence time was 20 min, the pore size was 0.1232 μm, which was about 8.45% higher than that with 10 min residence time. However, Zhao et al. (2018)'s results showed that this parameter had little effect on the pore size. In general, the relationship between BC properties and pyrolysis conditions needs to be further systematically explored.

HTC is a thermochemical conversion technique that can be directly applied to biomass with high moisture (sewage sludges, manures) or achieved by mixing water and biomass (rich in cellulose, lignin) to produce water-soluble organic matter and carbon-rich solid products under moderate temperatures (150–350 °C) and autogenous pressures (Sevilla and Fuerteshe 2009; Gascó et al. 2018; Wang et al. 2018). Similarly, the physicochemical properties of production (hydrochar) were affected by process parameters, such as temperature and feedwater pH value (Li et al. 2018b; Wang et al. 2018; Kochermann et al. 2018). Previous work by Gascó et al. (2018) suggested that higher temperatures would decrease the yields, H/C, and O/C rations, and lower H/C and O/C rations indicated higher content of aromatic compounds and carbon stability. The higher temperatures lead to the secondary decomposition of the solid residue and convert condensable products into non-condensable gas products (Wang et al. 2018). This phenomenon was consistent with Parshetti et al. (2013). Reza et al. (2015) showed that the hydrochar composition and chemical components in the HTC process varied with the pH of the feedwater. Compared with alkaline conditions, hydrochar prepared under acidic conditions had a larger specific surface area, higher cellulose and carbon elements, and lower hemicellulose and pseudolignin. However, under alkaline conditions, organic acids increased, while sugars decreased, and high pH resulted in a higher H/C ratio of the hydrochar (Funke and Ziegler 2010). Derived from the same biomass, hydrochar has a more aliphatic structure, lower carbon contents, and higher oxygen contents, and it has a more aromatic structure and higher thermal stability (Sun et al. 2014). Lower carbon contents and higher oxygen contents resulted in higher O/C and H/C ratios, which could better remove pollutants after further oxidation. In summary, BC with different characteristics can be prepared by changing biomass, production method and condition parameters to meet environmental applications.

3 The preparation of biochar-based composites

Due to the limitations of the pristine BC confining the application in environmental remediation, a growing number of investigations have been carried out to produce BC-based composite materials, which not only improved the physicochemical properties of BCs but also obtained a new composite combine the advantages of BCs with other materials. BC-based composite materials enhanced their performance by loading inorganic/organic materials on BC by physical, chemical, and other methods. BC-based composites can be divided into BC-magnetic composites, nano-metal oxide/hydroxide BC composites, and other types of functionalized BC (Huang et al. 2019).

3.1 Biochar-magnetic composites

For the low density and small particle size of BC, it is difficult to recover after large-scale sewage treatment and may arouse secondary pollution to water. BC-magnetic composites (MBC) can easily be separated and recycled from water by applying magnetic fields. The common preparation methods for MBC are liquid phase precipitation, impregnation, liquid phase reduction, and ball milling (Fig. 1 for details), and the synthesis methods of magnetic biochar with different biomass are summarized in Table 4.

The liquid precipitation method needs to prepare of BC at first, then mix the BC with Fe^{3+}/Fe^{2+} salt solution to form a suspension. After that, add NaOH solution dropwise while stirring at room temperature, then precipitation occurred (Mohan et al. 2015). Machinery may be the simplest method to prepare MBC (Thines et al. 2017). Mohan et al. (2013) successfully prepared MBC using this method (Fig. 1a for details). Wang et al. (2017) also synthetized MBC via this method and Fe_3O_4 particles were successfully loaded onto BC. MBC showed excellent performance in acid orange 7 (AO7) removal and satisfactory stability in a broad pH range. The impregnation method immerses biomass powder in the Fe^{3+}/Fe^{2+} salt solution or co-precipitate the Fe^{3+}/Fe^{2+} by chemicals before pyrolysis or microwave heating (Chaukura et al. 2017). In this way, a novel MBC derived from a peanut hull was made by Han et al. (2016) (see Fig. 1b). The obtained MBC had a potential for recycling by applying magnetic fields (saturation magnetization (Ms) up to 36.79 emu/g) and exhibited a higher ability to adsorb Cr(VI) than the original BC. The reduction method is to inject $NaBH_4/KBH_4$ solution into mixed solution of BC and Fe^{3+}/Fe^{2+} salt under nitrogen purging to reduce Fe^{3+}/Fe^{2+} into Fe^0 (see Fig. 1c). Quan et al. (2014) used this method to synthesize
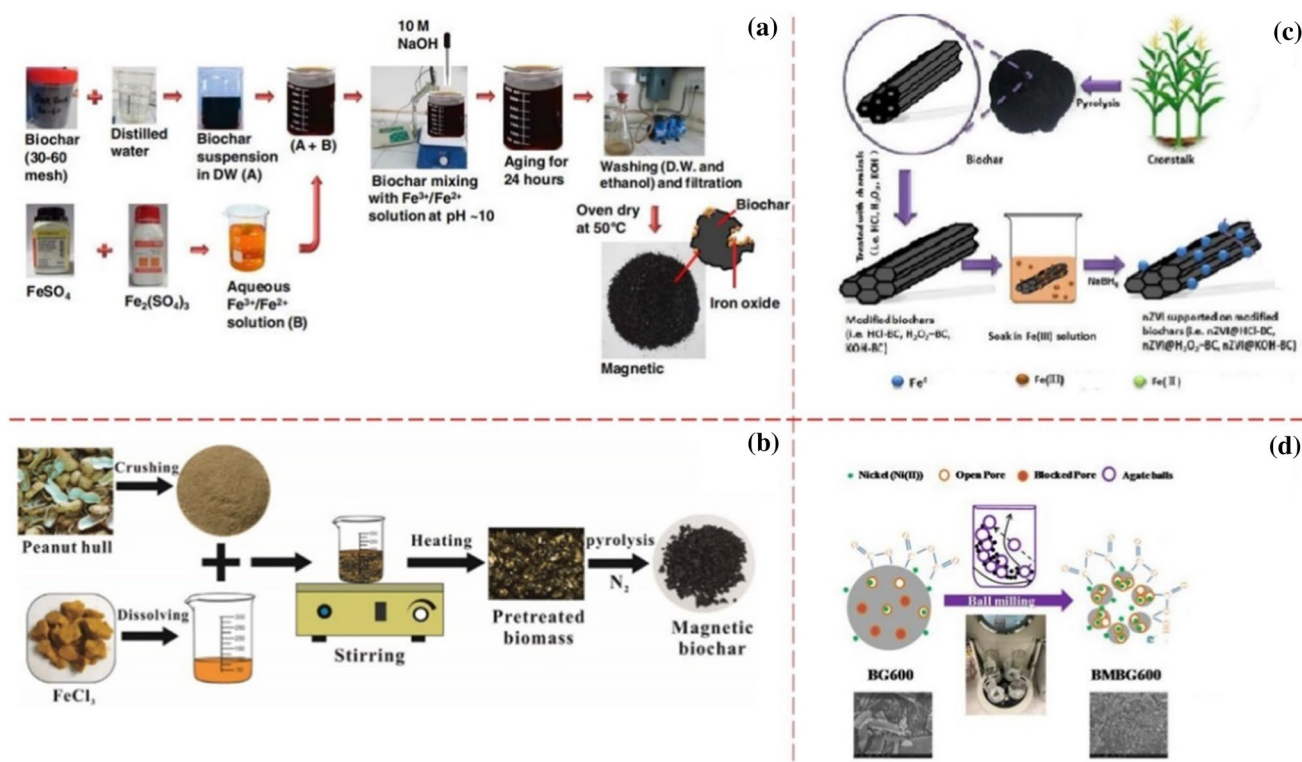
Fig. 1 Method of preparing magnetic biochar: The liquid precipitation method **a** (Mohan et al. 2013). The impregnation method **b** (Han et al.2016). Method of preparing magnetic biochar: The reduction method **c** (Dong et al. 2017). Ball milling **d** (Lyu et al. 2018)

nanoscale zero-valent iron BC composite (BC-nZVI), and the nZVI was dispersed on the BC surface without obvious aggregation. The degradation efficiency of AO7 by BC-nZVI reached 98.3% within 10 min. Apart from the above, mechanical ball milling is an efficient method and was widely used to produce large-scale MBC composites. These MBC samples were synthesized at room temperature using a planetary ball milling machine contained BC, iron or iron oxides and agate jars (see Fig. 1d). Ball milling MBC samples possessed higher external and internal specific surface area and acidic surface functional groups, which exhibited extraordinary adsorption capacity in removing Ni(II) from aqueous solutions (Lyu et al. 2018).

BC-magnetic composites were good methods to separate BC from aqueous solutions. The MBC made by the reduction method was rich in nZVI and had a good removal efficiency of contaminants. However, this method required the introduction of a protective gas (such as N_2) and hydrogen gas was generated during the preparation process. Moreover, nZVI has high activity, is easy to oxidize, and difficult to preserve, which limited its application. Furthermore, the ball milling method needs a ball milling machine with large volume and single function. Generally, each method has its own merits and demerits,

and the selection of suitable preparation methods should be considered comprehensively.

3.2 Nanometallic oxide/hydroxide biochar composites

The new composite materials produced by BC and nanomaterials (such as MgO and TiO_2) can significantly improve the surface functional groups, active sites, and catalytic degradation capabilities (Banat et al. 2000). Therefore, the synthesis of BC-based nanocomposites is a promising method, which can be widely used in environmental remediation. Nanometallic oxide/hydroxide BC composites can be divided into three types in preparation processes, including bioaccumulation of target elements, pretreatment biomass by metal salts, and insertion of metal oxide nanoparticles after pyrolysis (Banat et al. 2000; Huang et al. 2019).

Bio-accumulation target element is to enrich the target element in soil and fertilizer when planting biomass. The target element will bioaccumulate on biomass, which makes BC rich in the target element after pyrolysis. Li et al. (2018a) synthesized ZnO/ZnS modified BC by pyrolysis of zinc-contaminated corn stover obtained by the biosorption process. The ZnO/ZnS- BC has a larger specific surface area (397.4 m^2/g) than common BC (102.9 m^2/g), and the

Table 4 The Synthesis methods of magnetic biochar with different biomass

Biomass	Synthesis method	Iron species	Contaminants	References
Pineapple peel	Pyrolysis of biomass pre-treated with $FeCl_3$	ZVI and γ-Fe_2O_3	Cr(VI)	Shakya and Agarwal (2019)
Eucalyptus wood and poultry litter	Added biomass into a solution containing ferrous chloride and ferric chloride, then added NaOH solution to raise pH to 10, finally centrifuged the suspension and pyrolyzed	Fe_3O_4	Heavy metals (Cd, Cu, Zn and Pb)	Lu et al. (2017)
Pinewood	Nature hematite-treated biomass was pyrolyzed in a tube furnace	γ-Fe_2O_3	As(V)	Wang et al. (2015b)
Corn straw	Pyrolysis of mixed solution of $Fe(NO_3)_3$,$Mn(NO_3)_2$, egg white and biomass	$MnFe_2O_4$	Pb(II) and Cd(II)	Zhang et al. (2019a)
U. pinnatifida root	The biomass pretreated with $MgCl_2$ and $FeCl_3$ was processed by hydrothermal carbonization and the pH was adjusted to 10 with NaOH solution	$MnFe_2O_4$	Pb(II), Cu(II), and Cd(II)	Jung et al. (2018)
Coconut, pinenut and walnut shell	BC and stainless steel vials are stirred in a ball mill machine	Fe_3O_4	Carbamazepine and tetracycline	Shan et al. (2016)
Rice straw	Using liquid phase reduction method, drop KBH_4 into the mixed solution of BC and $FeSO_4$ under the protection of N_2	nZVI	Cr(VI)	Qian et al. (2018)

nano ZnO/ZnS are evenly distributed on the surface of BC. ZnO/ZnS-BC showed a strong adsorption ability to Pb(II), Cu(II), and Cr(VI), the maximum adsorption capacities were 135.8, 91.2, and 24.5 mg/g, respectively, which were much higher than pristine BC (63.29, 27.05, and 15.23 mg/g, respectively). This indicated that the nanometallic oxide BC made from contaminated-biomass may be an effective and economical method, which was helpful for waste utilization and environmental management. The metal salt pretreatment biomass is similar to the impregnation method in the MBC preparation. After immersing the target metal salt solution into BC, metal ions attach to the biomass surface and interior, and then the metal ions change into nano-metal oxides/hydroxides on BC after pyrolysis. The combination of nano metal oxides/hydroxides can endow BC with other functions to improve the application potentials. For instance, Lawrinenko et al. (2017) pretreated the biomass with iron and aluminum trichloride then obtained BC by slow pyrolysis. Al–O–C and Fe–O–C structures were formed on the surface, which facilitated wider distributions of metal atoms on BC. The oxyhydroxide coating on the surface can increase the points of zero net charge and thus increase anion exchange capacity. After pyrolysis, target metal oxide nanoparticles were inserted into the surface and inner pore by impregnation, evaporation, and heat treatment. For instance, Cope et al. (2014) used evaporation to modify BC by iron oxide to remove arsenic from water; the surface area and adsorption capacity of arsenate were 2.5 and 2 orders of magnitude higher than the pristine BC. Liang et al. (2017) immersed BC into $KMnO_4$ solution under vigorous stirring at room temperature; then Mn(II) acetate tetrahydrate was introduced to generate MnO_2-BC. MnO_2-BC showed an excellent adsorption performance for Cd(II) and Pb(II) removal.

3.3 Other types of functionalized biochar

Other types of functionalized BC mainly include heating/gas (steam, CO_2, etc.) activation, acid/alkali modification, and functional nanoparticles coated with BC. Steam activation is the most common method used in physical activation, which can increase the specific surface area and improve the adsorption capacity. For instance, Chakraborty et al. (2018) removed ibuprofen from aqueous solutions by steam-activated BC. The specific surface area after activation increased from 4.4 to 308 m^2/g, and the removal rate increased from 90 to 95%. Moreover, Azargohar and Dalai (2008) reported that

the specific surface area of steam-activated BC increased with the increase of steam temperature.

Acid/alkali (HCl, H_2SO_4, KOH) modification is a sort of chemical modification. Both acid and alkaline modifications can improve the physical and chemical properties and removal rate of BC. For example, Luo et al. (2018) used KOH modified BC to remove norfloxacin (NOR), sulfadiazine (SMR), and oxytetracycline (OTC). The surface area increased from 75.3 to 128.42 m^2/g and the removal rates of NOR, SMR, and OTC were all significantly enhanced. Andrew et al. (2016) used H_2SO_4, HNO_3, and a mixture of both to acidify BC, the functional groups (nitro and carboxyl) and the oxygen:carbon ratio of acidifying BC samples both increased, indicating that chemical oxidation of BC occurred after acid treatment. However, the thermal stability of BC might be reduced for the potential damage of graphite structures after acidification.

The common functional nanomaterials include graphene (GO), chitosan and graphitic carbon nitride (g-C_3N_4), etc. adding functional nanoparticles to BC can change the physicochemical properties and improve the ability of water treatment. The preparation of functional nanomaterials also can include pretreated biomass and post-processing of BC. Tang et al. (2015) made BC–GO nanocomposites by pretreating biomass, which was used to remove phenanthrene and mercury in aqueous solutions. It demonstrated that GO was mainly covered on the BC by *p–p* interaction, which made BC have a larger specific surface area and higher thermal stability. Therefore, the removal efficiency of phenanthrene and mercury has also been improved. However, Liu et al. (2015) prepared BC@g-C_3N_4 via mixing BC and melamine, which was then pyrolyzed at 300 °C for about 2 h. BC@g-C_3N_4 was used to remove cationic dye methylene blue (MB), anionic dye methyl orange (MO), and nonionic compounds (p-nitrophenol). The removal efficiency of cationic dye methylene blue (MB) by pure g-C_3N_4 was negligible but was significantly improved by BC@g-C_3N_4. This enhancing phenomenon also was observed in the removal of p-nitrophenol. But the removal of anionic dye methyl orange (MO) was not improved by BC@g-C_3N_4 since the negative charge on the BC@g-C_3N_4 surface inhibited the adsorption of anionic dyes on the BC@g-C_3N_4 surface. As is known to all, g-C_3N_4 is an active photocatalyst located in ultraviolet and visible light. Under illumination and irradiation, BC@g-C_3N_4 can significantly improve the decolorization of all samples. Furthermore, BC is a conductive material that acts not only as an electron transfer channel and acceptor to improve the separation of photogenerated electron–hole pairs, but also as a cocatalyst to provide sufficient catalytic sites for photocatalytic degradation. BC has a strong affinity for organics and makes them accumulate on the surface. However, the adsorption capacity of BC has some limitations and the regeneration of BC is difficult, which limited

the application of BC in water treatment. Adding g-C_3N_4 to BC to form BC@g-C_3N_4 can maintain and improve the ability of purification in the natural environment. Table 5 displays some biochar-based composites and their applications in water treatment for detail.

The BC-based composites combine the advantages of BC with nano-materials but we cannot ignore their potential risks. Recently, Luján et al. (2019) assessed the environmental impacts of GO and rGO and confirmed that the production of rGO will lead to electricity consumption and pollutant emissions (such as hydrazine, nitrogen oxide), which will lead to human toxicity cancer, human toxicity non-cancer effects, and freshwater ecotoxicity. Furthermore, ZnO has been widely applied in wastewater treatment due to the low cost, chemical stability and photocatalytic performance. However, ZnO nanoparticles (nZnO) released into the environment may pose a serious threat to human health. For instance, Wahab et al. (2013) reported that the melanoma cancer cells produced reactive oxygen species (ROS) and apoptosis after contact with nZnO. Likewise, nZnO will cause dramatic damage to neural stem cells when the concentration rises higher than 12 ppm after 24 h exposure, which may be attributed to the dissolved Zn^{2+} in the cultivation environment or inside cells (Deng et al. 2009). In conclusion, the preparation of BC-based composites should consider the removal efficiency and the potential risk to the environment.

4 Removal of heavy metal contaminants

Heavy metals are not biodegradable and tend to accumulate in living organisms through the food chain. Long-term exposure to heavy metals can lead to endocrine disorders, cancer, and other diseases and pose a serious threat to human health. BC can effectively remove metal ions by adsorption, ion exchange, electrostatic interaction, complexation, precipitation, etc. (Inyang et al. 2016).

4.1 Removal of inorganic contaminants by biochar

Recently, Komkiene and Baltrenaite (2016) selected the silver birch as a carbon source to prepare BC, and then investigated the adsorption performance of BC towards Cu(II) and Zn(II) at different water environmental condition. The results showed that the maximum adsorption capacities of Cu(II) and Zn(II) reached up to 128 μg/g and 107 μg/g, respectively, which indicated that BC was a promising adsorbent to remove of heavy metals from the contaminated water. The BC was prepared by pyrolysis of water hyacinth at different temperatures (250–550 °C) and applied for the removal of Cd(II) ions from wastewater. BC450 (produced at 450 °C) showed a good removal

Table 5 Biochar-based composites and their applications in water treatment

Biomass	Functional nanomaterials	Contaminants	Strategies applied	Characteristic and advantages	Effect on the removal performance	References
Waste walnut shell	TiO_2	Methyl orange	Pyrolysis of Tetrabuty lorthotitanate pretreated biomass	Strong interaction between BC and TiO_2 effectively promotes the transfer of photogenerated electrons in TiO_2	The decolorization rate reaches 96.88% and still have high activity after 5 catalytic cycles	Lu et al. (2019)
Wood	Go	Phthalic acid esters	Biomass is immersed into the GO suspension, then pyrolysis of mixture	Higher surface area, porous structure and thermal stability	More efficient removal of organic pollutants through $\pi-\pi$ EDA interaction and the maximum adsorption capacity was 30.78 mg/g	Abdul et al. (2017)
Wheat straw	CeO_2	Reactive Red 84	CeO_2 synthesized by hydrothermal method, then loaded on BC	Higher surface area, average pore size and pore volume	High removal efficiency (95.8%) and still have 87% after 5 catalytic cycles	Khataee et al. (2018)
Corn stover	ZnO/ZnS	Pb(II), Cu(II) and Cr(VI)	Pyrolysis of zinc loaded biomass	Well-developed porous structure in terms of high BET surface area and total pore volume	More efficiency than the common BC, the maximum adsorption capacities were 135.8, 91.2 and 24.5 mg/g	Li et al. (2018a)
Rice husk	S-nZVI	Nitrobenzene	Liquid phase reduction of Fe^{2+} impregnated BCs, while adding $Na_2S_2O_4$ to form BC-S-nZVI	S-nZVI particles are dispersed on the BC surface and channels, effectivelyprevented the agglomeration of S-nZVI particles	The excellent reducibility of S-nZVI@BC (q_m = 588.23 mg/g), the removal efficiency after 5 cycles is 72%	Zhang et al. (2018)
Rice husk	Fe_3O_4	U(VI)	Calcining the mixtures of siderite and rice husk	A amount of nanoparticles were attached on the surface of BCand presents a superior magnetic response	Displayed a preeminent adsorption performance for U(VI) compared to other adso rbents (q_m = 52.63 mg/g).	Li et al. (2018c)
Corn straw	MnO_x	Cu(II)	Pyrolysis of BC pretreated $KMnO_4$	BC was covered with manganese oxide and average pore was increased	8 times higher than pure BC, the highest adsorption capacity is 160 mg/g	Song et al. (2014)
Agricultural straw	$g-MoS_2$	Tetracycline	Hydrothermal treatment of Na_2MoO_4 and BC	MoS_2 nanosheets were dispersed on the surface of BC	Maximum adsorption capacity was 249.45 mg/g, and remains high adsorption capacity after five adsorption cycles	Zeng et al. (2019)

Fig. 2 The schematic illustration of Cr(VI) removal mechanisms **a** on the surface of BC (Vo et al. 2019), **b** on the surface of modified BC (Zhang et al. 2020a)
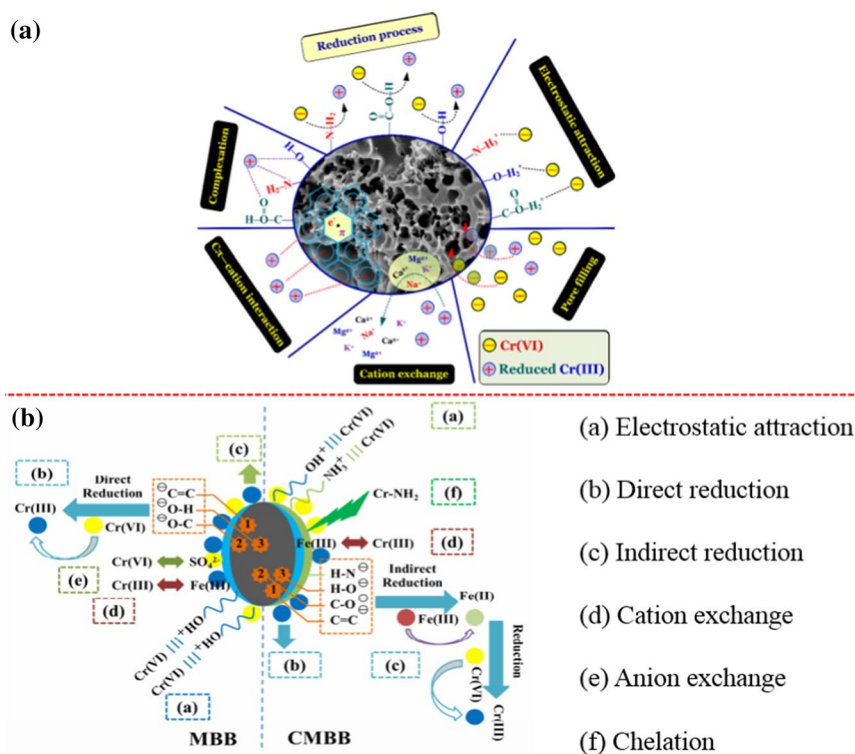
efficiency (almost 100% Cd(II) from the aqueous solution within 1 h). Moreover, Rafique et al. (2019) found that compared with the control soil, BC stemming from jujube leaves and manure waste pyrolyzed at 700 °C showed the highest reductive efficiency of soil soluble Cr (93%) and the concentrations of leachates were reduced by 59%. Likewise, the BC produced from different biomass was used to immobilize Cd and Pb in soil, the concentrations of leachates were reduced by 3.28–71.01% (Xu et al. 2020). Furthermore, the accumulation in roots, stems, and leaves was significantly decreased (45.43–99.28%).

Cr(VI) as the most common heavy metal-contaminant has various removal of mechanisms, such as electrostatic attraction, direct reduction, and complexation. The schematic illustration of Cr(VI) removal mechanisms on the surface of BC is shown in Fig. 2a. Direct reduction is the main removal mechanism for Cr(VI) removal by BC. The X-ray absorption near edge structure (XANES) analyses of BC before and after reaction showed that there did not exist trivalent Cr(III) in the spectrum of Cr(VI) sample before the reaction with BC. However, the peak of Cr(VI) was decreased, while the peak of Cr(III) was increased after the reaction, which indicated that most of Cr(VI) was reduced to Cr(III) (Rajapaksha et al. 2018). In addition to direct reduction, electrostatic attraction is another mechanism for Cr(VI) adsorption by BC. Zhou et al. (2016) used BC stemming from ramie residues at different temperatures to remove Cr(VI) in aqueous solutions. The

removal efficiency decreased with the increase of the initial pH value. At pH 2, the pH value of zero charge point (pH_{PZC}) > pH, the BC surface was positively charged and some functional groups (hydroxyl and carboxyl groups) were protonated, which electrostatically were attracted by the Cr(VI) ions. Besides, the Fourier transform infrared spectrophotometer (FTIR) spectrums of BC samples before and after reaction with Cr(VI) showed that the disappearance of the C=O stretching band at 1734 cm^{-1} and the decrease of the peak intensity at 1270 cm^{-1} (phenolic hydroxyl group) indicated the carboxyl and hydroxyl groups in the BC played an important role in the adsorption of Cr(VI). Furthermore, both Cr(III) and Cr(VI) were detected in aqueous solutions and on the BC surface, which may be attributed to the complexation of BC functional group and Cr(III) to keep part of Cr(III) on the surface and the remainder discharged into aqueous solution. Similar results had been reported by Dong et al. (2011). Vo et al. (2019) have proposed the removal mechanism of Cr(VI) by carbonaceous porous materials (BC and activated carbon) involving pore filling, π-cation interaction, and cation exchange. The removal of inorganic pollutants from aqueous solution by biochar is summarized in Table 6. The Q_{max} of inorganic pollutants removal by the pristine BC ranged from 7×10^{-3} to 161.9 mg/g.

Table 6 Removal of inorganic pollutant from aqueous solution by biochar

Biomass	Contaminants	pH	Q_e (mg/g)	Q_m (mg/g)	Removal rate (%)	References
Peanut shell	Pb(II)	5.0	51.9	52.8	46.1	Wang et al. (2015c)
Chinese medicine material residue	Pb(II)	5.0	82.3	82.5	73.2	Wang et al. (2015c)
Rice straw	Eu(III)	3.0	4.9	98.0	58.7	Zhu et al. (2018a)
Hickory chips	Hg(II)	6.0	5.0	–	75.0	Xu et al. (2016)
Pine cones	As(III)	4.0	4.0×10^{-3}	7.0×10^{-3}	40.0	Van et al. (2015)
Ficus microcarpa Aerial root	U(VI)	4.0	20.7	–	69.0	Li et al. (2019b)
Corn stover	U(VI)	5.0	74.8	111.5	74.8	Li et al. (2019a)
Artemisia argyi stem	Cu(II)	7.0	18.7	156.0	74.8	Song et al. (2019)
Artemisia argyi stem	Cr(VI)	1.0	15.8	161.9	63.2	Song et al. (2019)
Ramie residues	Cr(VI)	2.0	31.8	61.2	63.6	Zhou et al. (2016)

4.2 Removal of inorganic contaminants by biochar-based composites

Recently, Wang et al. (2015a) used 3.65% Mn to impregnate the BC to enhance the removal of lead. The removal rate of lead increased from 6.4% to 98.9% at pH 5.0. This improvement can be attributed to the increase of hydroxyl groups and the decrease of the pH_{PZC}. The maximum adsorption capacity of modified BC at 298 k is five times that of the pristine BC and the adsorption rate is faster. Furthermore, Tan et al. (2016) prepared BC and modified it with Na_2S and KOH for Hg(II) adsorption. The adsorption rate increased significantly by 76.95% and 32.12%, respectively. The increase of specific surface area from 32.85 m²/g (pristine BC) to 55.58 (Na_2S@BC) or 59.23 m²/g (KOH@BC) after modification

can be ascribed to the removal of coal tar accumulated in the pore. Na_2S@BC can form HgS precipitates with Hg(II), which is another effective way to improve the Hg(II) removal rate. Li et al. (2019b) prepared $KMnO_4$ modified BC and applied it for U(VI) removal. The increase of oxygen-containing functional groups and the production of MnO_2 nanoparticles caused by the modification of $KMnO_4$ significantly increased the U(VI) adsorption capacity through coordination and Lewis acid–base interaction. Furthermore, Fan et al. (2020) embedded nZVI on BC by one-pot pyrolysis of sawdust and Fe_2O_3 mixture to improve the ability of As immobilization. Compared with pristine BC treatment, the mobility of As in soil decreased. This phenomenon may be due to the adsorption and co-precipitation of As by the corrosion production (amorphous FeOOH) of nZVI on the

Table 7 Removal of inorganic pollutants from aqueous solution by biochar-based composite materials

Biomass	Modification method	Contaminants	Q_e (mg/g)	Q_m (mg/g)	Removal rate (%)	References
Ficus microcarpa aerial root	MnO_2	U(VI)	24.6	–	82.0	Li et al. (2019b)
Water hyacinth	Graphene oxide	Cr(VI)	47.8	150.0	95.6	Shang et al. (2016)
Corn straw	$MnFe_2O_4$	Pb(II)	80.4	154.94	99.0	Zhang et al. (2019a)
Leaf litter	CeO_2, MoS_2 and magnetic	Pb(II)	24.9	263.6	99.6	Li et al. (2018d)
Peanut hull	Zero valent iron	Cr(VI)	223.2	–	100.0	Liu et al. (2019c)
Lufa cylindrica fiber	MnO_2	U(VI)	–	904.0	100.0	Ioannou et al. (2019)
Pinus massoniana	Manganese-oxide	Pb(II)	91.7	121.8	98.9	Wang et al. (2015a)
Carbonaceous biomass	ZnS and magnetic	Pb(II)	262.4	367.7	100.0	Yan et al. (2015)
Corn straw	Ferromanganese binary oxide	Cu(II)	71.4	64.9	100.0	Zhou et al. (2018)
Corn straw	Ferromanganese binary oxide	Cd(II)	100.0	101.0	100.0	Zhou et al. (2018)
Municipal solid waste	KOH	As(V)	33.2	31.0	100.0	Jin et al. (2014)
Rice husk	MnO_x	Pb (II)	60.7	86.5		Faheem et al. (2016)

surface of BC. Furthermore, most As(V) was reduced to As(III) after adsorption by nZVI-BC. Similarly, Gao et al. (2020) co-pyrolyzed the mixture of rape straw and KH_2PO_4 to prepare BC and the BC displayed a high immobilization capacity to heavy metals (Pb, Cu, and Cd). This may owe to the direct complexation and precipitation of heavy metals with phosphate and –OH on the surface of BC or indirectly enhancing the immobilization of heavy metals by increasing the pH value and available P of soil. Besides, the removal of inorganic pollutants from aqueous solution by biochar-based composite material is summarized in Table 7. The Q_{max} of inorganic pollutants removal by BC-based composites ranged from 31 to 904 mg/g. Biochar-based composites combine the advantages of BC with other materials, and the removal efficiency have been significantly improved.

Zhang et al. (2020a) used chitosan-modified magnetic BC to enhance the Cr(VI) removal from the aqueous solution, and the maximum adsorption capacity increased from 75.8 mg/g to 127 mg/g. Compared to the ordinary BC, Fe–O stretching was observed on magnetic BC (MBC) and chitosan-modiied MBC (CMBC), and combined with XRD spectra, it was indicated that Fe_3O_4 was successful loaded on the BC. Contrasting the FTIR spectra before and after reaction, the C=O, C–O, Fe(III)-O, and H–O changed, which indicated that all of those participated in the reaction process. On the one hand, the aforementioned group can serve as an electron-donating in the reduction of Cr(VI). On the other hand, this group can form a complexation between Cr(VI) and CMBC/MBC surface group. Furthermore, electron-donating can provide electrons to reduce Fe(III) to Fe(II); then Fe(II) as a reductant indirectly reduced Cr(VI) to Cr(III). Furthermore, the chitosan coating introduced –NH2, and the charge transfer between Cr(VI) and free −NH2, which interpreted the appearing N1s peak in the

FTIR spectra of Cr(VI) removal by CMBC. At low pH, -NH2 will form $-NH^{2+}$, $-NH^{3+}$ then via electrostatic attraction to remove the Cr(VI). In addition, Fe^{2+}/Fe^{3+} will exchange cations with Cr(VI). (Fig. 2b for details). Therefore, synthesizing biochar-based composites may be a feasible way to remove inorganic in aqueous solutions.

5 Removal of organic contaminants

Organic contaminants are common in wastewater. Recently, dyes, phenols, pesticides, and antibiotics have attracted much attention because of the complex aromatic structure, extreme toxicity, and biodegradable resistances in environments. Here, we have selected some representative examples to demonstrate the feasibility of BC and the superiority of BC-based composites to remove organic contaminants. And the removal rates of organic contaminants from aqueous solution by biochar and BC-based composites are summarized in Tables 8 and 9; the Q_{max} of organic pollutant removal by the pristine BC ranged from 10.4 to 610.1 mg/g, and the removal rates of organics by the BC-based composites have been significantly improved to more than 90%.

5.1 Removal of dye contaminants

Dyes are one group of organic contaminants, which are used extensively in textile, paper, and printing industries. Dyes have good solubility, complex aromatic molecular structures and are not easy to be degraded naturally. Colored dyes can be recognized by the human eye, significantly reduce light penetration into the water, and cause aquatic organisms to die from oxygen deprivation. Besides, dyes are rich in aromatics which are toxic to organisms and

Table 8 Removal of organic contaminants from aqueous solution by biochar

Biomass	Contaminants	pH	Q_e (mg/g)	Q_m (mg/g)	Removal rate (%)	References
Dairy manure	Atrazine	–	0.8	–	39.9	Cao and Harris (2010)
Corn stover	Methylene blue	11.0	201.6	349.7	25.2	Li et al. (2019a)
Food waste	Phenol	3.0	9.8	14.6	65.2	Lee et al. (2019)
Cattle manure	Methylene blue	–	161.3	242.0	97.5	Zhu et al. (2018b)
Kelp seaweed and spent mushroom substrate	Crystal violet	6.0	562.6	610.1	14.1	Sewu et al. (2017)
Pine fruit shell	Phenol	6.5	9.9	10.4	19.8	Mohammed et al. (2018)
Pine fruit shell	Phenol	6.5	16.0	16.0	31.9	
Pine fruit shell	Phenol	6.5	26.5	26.7	52.9	
Eucalyptus bark	Methylene blue	11.3	90.1	104.2	36.8	Dawood et al. (2016)
Pine wood	Salicylic acid	2.5	10.0	22.7	40.0	Essandoh et al. (2015)
Pine wood	Ibuprofen	3.0	10.4	10.7	41.7	
Rice straw	Tetracycline	–	28.5	50.7	56.9	Fan et al. (2018)

Table 9 Removal of organic contaminants from aqueous solution by biochar-based composite materials

Biomass	Modification method	Contaminants	pH	Q_e (mg/g)	Q_m (mg/g)	Removal rate (%)	References
Paper mill sludge	ZVI	Pentachlorophenol	7.0	40.2	–	100.0	Devi and Saroha (2014a)
Chestnut leaf	g-C$_3$N$_4$	Methylene blue	–	10.9	–	91.0	Liu et al. (2015)
Paper sludge and wheat husk	TiO$_2$	Reactive blue 69	7.0	13.0	–	97.5	Khataee et al. (2017)
Wheat straw	Ni/Fe bimetallic	1,1,1-trichloroethane	6.0	198.6	–	99.3	Li et al. (2017b)
Palm kernel	Magnetic	Phenol	8.0	3.2	10.84	93.4	Hairuddin et al. (2019)
Rice husk	S-nZVI	Nitrobenzene	7.0	550.0	588.2	100.0	Zhang et al. (2018)
Waste walnut shell	TiO$_2$	Methyl orange	–	77.5	–	96.9	Lu et al. (2019)
Carbonaceous	ZnO	Gemifloxacin	5.5	12.8	-	96.1	Gholami et al. (2019)
Orange peel	Magnetite	Naphthalene	–	18.0	24.0	99.6	Chen et al. (2011)
Algal	SiO$_2$	Phosphate	5.0	49.7	159.4	98.0	Wang et al. (2016a)
Carbon-rich biomass	AlOOH	Phosphate	–	44.5	135.0	100.00	Zhang et and Gao (2013)

further cause deterioration of water. Therefore, it is urgent to find an eco-friendly, low-cost, and effective method to treat dyes wastewater.

5.1.1 Removal of dye contaminants by biochar

According to the literature, BC has been widely used in the water treatment of dye. For example, Qiu et al. (2009) prepared BC to remove reactive brilliant blue (KNR) and Rhodamine B (RhB) from aqueous solutions. The electrostatic interaction between RB and BC, and the protonation of RB make the BC have an obvious adsorption effect on RB. As it is known to all, the adsorption mechanisms of MB by BC include electrostatic interaction, ion exchange, and hydrogen bond interaction. Fan et al. (2017) used municipal sludge to prepare BC to remove methylene blue (MB), which was accurately described by a pseudo-second-order model and obtained a good adsorption effect (up to 100%). Moreover, the removal rate of MB was still 60% after three cycles. During the adsorption process, the removal rate and adsorption amount increased with the increase of pH, which might be ascribed to electrostatic interaction. Besides, Si–O–Si on BC can provide adsorption sites and can interact n-π with the nitrogen functional groups of MB. Furthermore, MB can form hydrogen bond interactions with the hydrogen of BC.

5.1.2 Removal of dye contaminants by biochar-based composite materials

BC can effectively adsorb contaminants in water, but there are still some limitations of the pristine BC which cannot meet the practical application. Therefore, the BC-based composites have attracted the attention of many scholars. For example, Khataee et al. (2017) reported the ultrasound-catalyzed degradation of RB69 by TiO$_2$-BC. TiO$_2$-BC displayed a large specific surface area and pore volume which could exhibit high acoustic catalytic performance for RB69 degradation. The removal efficiency of RB69 reached 98.1% by ultrasound/TiO$_2$-BC, which was higher than that by ultrasound/BC (63.8%). The presence of TiO$_2$ could increase the number of cavitation bubbles on the solid surface, thus increasing the mass transfer rate of RR84 molecules from liquid to catalyst surface and promoting the cracking of water molecules to produce more ●OH radicals. Furthermore, the surface of TiO$_2$-BC was positively charged in an acidic environment, which promoted the adsorption of anionic dyes and the decolorization efficiency of RB69 in acidic solutions. The mechanism of ultrasonic TiO$_2$-BC systems involving $^{\cdot}$OH, h$^+$ and $^{\cdot}$O$_2^-$, H$_2$O, and OH$^-$ can combine with h$^+$ to form $^{\bullet}$OH free radicals. When ethanol was used as $^{\cdot}$OH scavenger, the removal rate of the reaction system decreased

significantly, indicating that ⋅OH radicals were particularly important in the reaction system. After five cycles, the degradation efficiency was still 92.1%, and the durability and reuse of TiO₂-BC were relatively acceptable. Similarly, Lu et al. (2019) applied TiO₂-BC to remove methyl orange (MO); the decolorization rate was 96.88% and the mineralization rate was 83.23%.

5.2 Removal of phenol contaminants

Phenols are another sort of organic contaminants that can affect the taste of fish, shrimp, and drinking water at low concentrations. Phenols are harmful to the human body and have been classified as harmful pollutants (Banat et al. 2000). Phenols are rich in aromatic structure, have strong adsorption affinity, and are not easily degraded by

microorganisms. BCs are rich in porous structure which has a strong affinity for aromatic organic compounds, so BC can be selected to remove phenols contaminants in aqueous solutions.

5.2.1 Removal of phenol contaminants by biochar

Many researchers are committed to studying phenol removal by BC in water. Mohammed et al. (2018) used the BC prepared at different temperatures to remove phenol. The maximum adsorption capacity ranged from 10.373 to 26.738 mg/g and the removal rate reached 67–99%. Thang et al. (2019) prepared BC using chicken manure to remove the phenol and 2,4-Dinitrophenol (DNP) in the aqueous solution; phenol and DNP could be completely removed within 90 min. And BC still effectively removed about 80%
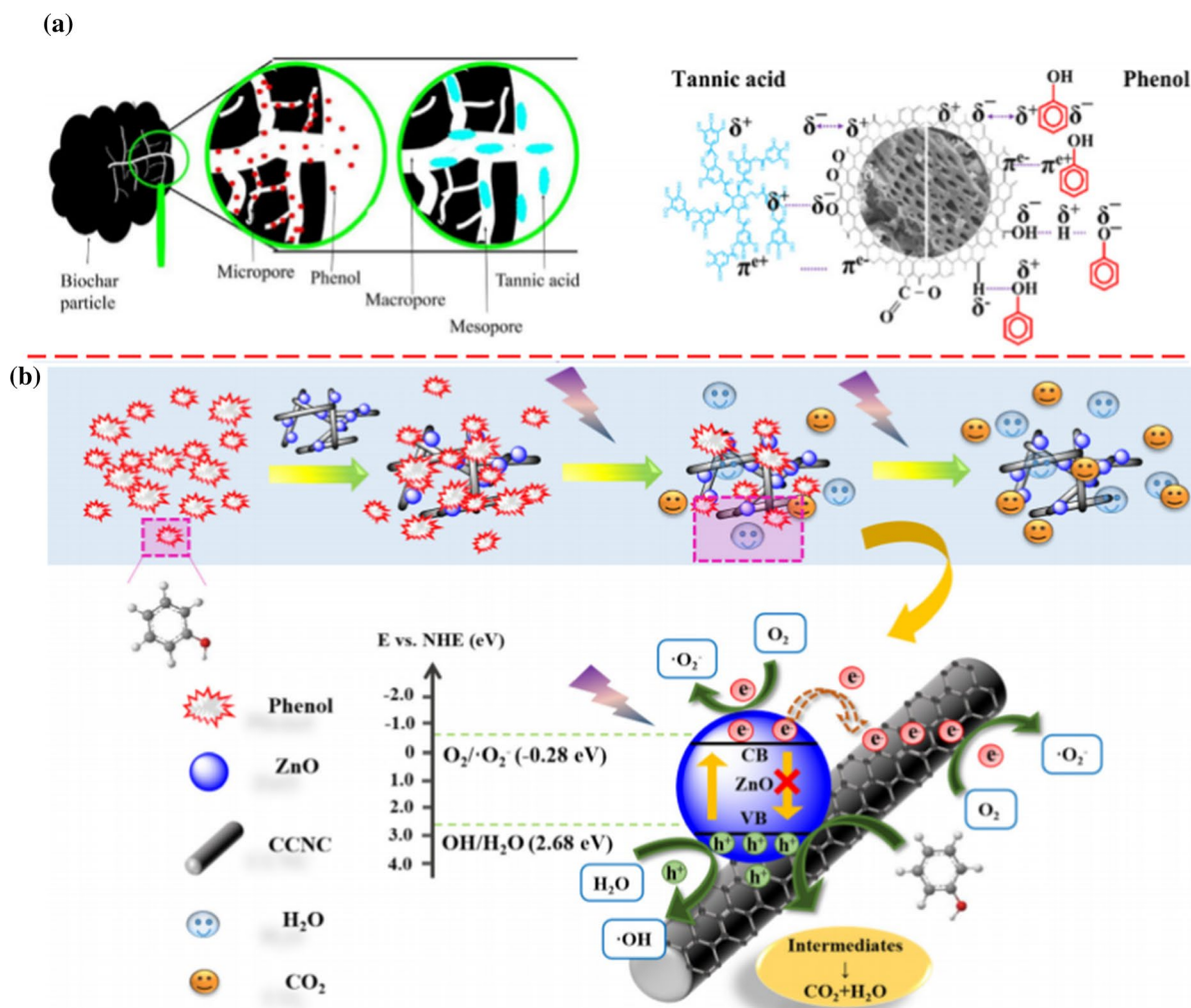
Fig. 3 **a** The mechanism of adsorption of phenol on the surface of BC (Lawal et al. 2021), **b** the mechanism of photocatalytic degradation for phenol induce by CCNC/ZnO (Zhang et al. 2020b)

of phenolic pollutants in field applications. The maximum adsorption capacity of BC for phenol and DNP were 106.2 mg/g and 148.1 mg/g, respectively, which were ascribe to the high surface area, rich in pore structure, and the large oxygen surface functional groups on BC. The removal mechanisms of phenols may be ascribed to electrostatic interaction, π–π interaction, and hydrogen bonding. Under neutral solution conditions, the BC surface is positively charged, while DNP and phenols are negatively charged due to electron-rich benzene rings. Thus, BC can easily remove phenols and DNP by electrostatic interactions. Oxygen-containing functional groups (such as -COOH, -OH) on the BC surface act as π- electron donors to adsorb phenols considered as the π-electron acceptor by π–π interaction. Moreover, hydrogen bonding is one of the strongest interaction mechanisms between BC and phenolic compounds by sharing electron pairs. And there are two main ways of hydrogen bond interaction: (1) the interaction between hydroxyl groups (H- donor) on the surface of BC and oxygen or nitrogen (H-acceptor) of phenols; (2) the interaction between hydroxyl groups on the surface of BC and aromatic rings of phenols. Finally, the BC has high reusability, and the loss of adsorption capacity for phenol and DNP is less than 20% after five cycles. Lawal et al. (2021) used BC made from oil palm leaves by steam pyrolysis to remove phenol; the adsorption capacity reached 62.89 mg/g for phenol and was well fitted with the Freundlich model ($R^2 = 0.9863$), and the mechanism of the phenol removal was illustrated in Fig. 3a. Phenol can access adsorption sites in micropore regions, then be adsorbed on the surface of BC through H bonds and π–π interaction. Thus, BC can be used as a promising adsorbent for treating wastewater containing phenol compounds.

5.2.2 Removal of phenol contaminants by biochar-based composite materials

The removal of phenols was the main research objective of BC-based nano-composites for the treatment of wastewater. Lisowski et al. (2017) prepared TiO$_2$-BC by using the ultrasound-assisted methodology and photocatalytic degradation of phenol in aqueous solutions. The degradation rate of phenol by TiO$_2$-BC coupled with UV reached 64.1% and 33.6%, respectively, which were much higher than that by original BC with UV and visible light (less than 6%). Besides, the physicochemical properties of the BC were significantly affected by the ultrasound-assisted methodology. The TiO$_2$-BC surface area increased from 254 to 399 m^2/g and was 65% larger than the TiO$_2$-BC prepared by ordinary methods. Ultrasonic treatments cause cracks in solids, resulting in more mesoporous structures and active sites and improving degradation efficiency. The combination of BC and TiO$_2$ can improve the light absorption ability

of visible light, effectively transfer photoinduced electrons, reduce the binding of e$^-$–h$^+$, and produce •OH and ·O$_2^-$. Furthermore, the TiO$_2$ and BC combination effectively improved the service life in the presence of ultrasound, and the loss of reactivity was only about 10% after 5 cycles. As a result, TiO$_2$-BC prepared by this method had high photocatalytic efficiency and good cycle stability. Furthermore, Zhang et al. (2020b) introduced ZnO into BC to remove phenol from aqueous solutions. The composites displayed good photocatalytic performance and satisfactory stability (95% photodegradation efficiency after 5 cycles). The ZnO was dispersed on the surface of BC, resulting in more active sites. Besides, ZnO could generate electrons (e$^-$)/holes (h$^+$) pairs under light irradiation. The e$^-$ from the valence band (VB) can be transferred to the surface of BC and react with the dissolved oxygen (O$_2$) to form superoxide radicals (·O$_2^-$). Meanwhile, the h$^+$ from the VB can be trapped by H$_2$O or hydroxyl groups and form hydroxyl radical (·OH). Finally, the phenol molecules reacted with ·O$_2^-$ and ·OH and further degraded to H$_2$O and CO$_2$. The specific degradation pathway of phenol is shown in Fig. 3b.

5.3 Removal of antibiotic contaminants

Considering the rapid development of the medical level, the content of drug active compounds in environments has increased significantly, becoming an important new contaminant (Rossner et al. 2009). Such contaminants are of great concern for human health and the ecological environment. Among these contaminants, antibiotics are not easily biodegradable; residual antibiotics will increase the resistance of aquatic microorganisms, and can cause serious impacts on the ecological environment through bioaccumulation and biomagnification (Zhou et al. 2009).

5.3.1 Removal of antibiotic contaminants by biochar

BC is rich in aromatic structure, and it was an excellent adsorbent for removing hydrophobic organics contaminants (Vithanage et al. 2015). Recently, Fan et al. (2018) pyrolyzed rice straw at different temperatures for the removal of typical antibiotics tetracycline (TC) by BC. The BC obtained at a higher temperature could possess the maximum adsorption capacity of 50.72 mg/g due to its large specific surface area, abundant aromatic structure and rich graphite carbon. The effect of pH during BC removal of TC was neglect (Liu et al. 2012), and the strong π–π interaction was the main mechanism in this adsorption process. Peiris et al. (2017) used BC to remove tetracyclines and explored their mechanisms in depth. The mechanisms were demonstrated in Fig. 4a including surface complexation, hydrogen bonding, cation bridging, and electron attraction.
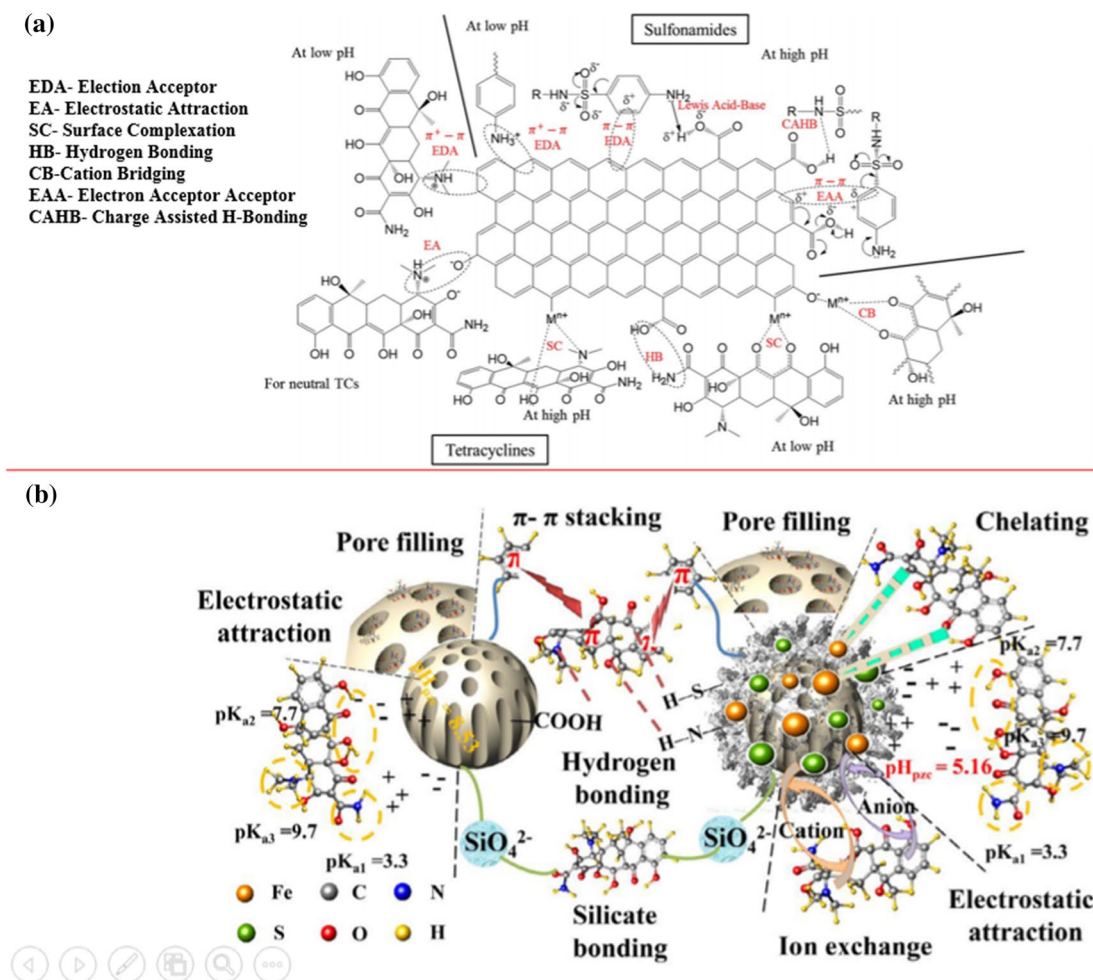
(a)

(b)

Fig. 4 **a** The mechanism of adsorption of sulfonamides and tetracyclines on the surface of BC (Peiris et al. 2017). **b** The mechanism of adsorption of tetracyclines on the surface of modified BC (Liu et al. 2019b)

Moreover, Rajapaksha et al. (2014) produced BC by an invasive plant at 700 °C to treat the sulfamethazine (SMT) contaminant soil. The results showed that BC can significantly reduce the absorption of SMT by lettuce (compared with the control, the SMT absorption was decreased by more than 63% after adding 5% BC). It may be attributed to the electrostatic cation exchange and the π–π electron donor–acceptor interaction between the protonated aniline ring of the SMT molecule and π-electron-rich surface on the BC, which promoted the adsorption of SMT by BC and decreased the bioavailability of SMT. Likewise, Yue et al. (2019) claimed that BC could effectively remove the antibiotics and their intermediates, and the removal rate of antibiotics increased by more than 10% compared with control. They found that the BC could alter soil properties, such as electrical conductivity, pH, C/N ratio, etc., thereby promoting the degradation of antibiotics by microorganisms. Furthermore, the introduction of BC can increase the carbon

supply and change the bacterial community by enhancing copiotrophic bacteria (Liu et al. 2020).

5.3.2 Removal of antibiotic contaminants by biochar-based composites

Lately, Huang et al. (2017) used bamboo sawdust as biomass to prepare a novel graphene oxide-coated BC nanocomposite (GO-BC) for the removal of SMT. The molar $(O + N)/C$ ratios represent the polarity of carbonaceous nanocomposites. The $(O + N)/C$ of pristine BC is relatively low, but BC-based composite material can significantly increase the $(O + N)/C$. Besides, C=O is the only form of the double bond of carbon to oxygen in the pristine BC, while O–C=O groups are the dominated double bonds of carbon to oxygen detected in the GO-BC. In addition, the analysis showed that about 30% of SMT was adsorbed by GO-BC due to the increasing surface functional groups.

Moreover, the specific surface area of GO-BC increased from 184.9 to 348.2 m^2/g and the adsorption capacity of SMT was two times higher than that of the original BC. It can be concluded that the larger surface area provided additional adsorption sites. The adsorption of SMT on BC and GO-BC was in good agreement with the pseudo-second-order model, indicating that the SMT was removed by the chemisorption process. Liu et al. (2019b) modified BC by chitosan and FeS$_x$ for the TC removal, and the results showed that the maximum capacity of TC removal by BC and modified BC were 51.78 and 193.01 mg/g, respectively. Figure 4b reveals the mechanisms of TC removal by chitosan-Fe/S-BC, including electrostatic attracting, π-π stacking, and pore filling. Compared with pristine BC, the removal mechanism after BC modification increased chelation and silicate bonding, and silicate bonding was one of the main removal mechanisms. Hence, BC has a good application prospect through modification.

5.4 Removal of pesticide contaminants

With the rapid industrialization and modern agricultural practices, pesticides are widely used in soil, the extensive and inefficient use of pesticides over the last several decades resulted in serious environment problem. The widespread application of pesticides has caused pollution of soil and water. As known to all, pesticides are persistent, toxic, and carcinogenic, which poses a serious threat to the environment and human health. Therefore, it is necessary to develop more efficient and reliable materials to remove pesticides from aqueous solutions.

5.4.1 Removal of pesticide contaminants by biochar

Zhang et al. (2013b) used pig manure as biomass to prepare BC350; BC700 at different temperatures for the removal of carbaryl and atrazine. The normalized sorption coefficient (K_{oc}) values were $10^{1.90}$–$10^{3.57}$ L/kg for atrazine and $10^{2.65}$–$10^{3.66}$ L/kg for carbaryl. The decomposition rates of carbaryl and atrazine by BC700 after 12 h were 71.8% and 27.9%, respectively. In this study, the ratios of H/C and (O + N)/C between BC350 and BC700 have no obvious difference, while BC700 has much higher ash content than BC350, which demonstrates that two pesticides can be adsorbed by mineral ash through specific interactions. After deashing, the removal rates of pesticides were significantly improved, which also indicated that high content of ash covered the organic groups and weakened specific interaction thereby reducing the removal rate. Moreover, the molecular size of atrazine was smaller than that of carbaryl. This finding indicated that the mechanism of the pore-filling effect plays an important role in pesticide removal. The published literature demonstrates the mechanisms of the removal of

pesticides by BC including hydrophobic interactions, pore filling, and specific interactions (Zheng et al. 2010).

Ali et al. (2019) pyrolyzed different biomass to prepare BC to investigate the bio-accessible of organochlorine pesticides (OCPs) and bio-accumulation in vegetables. The results indicated that selected BC could effectively reduce the bio-accessibility of OCPs (47–60%) and the concentration of OCPs in grown vegetables was decreased significantly (85–86%). The introduction of BC changed the microbial community structure, the relative abundances of *Acidobacteria*, *Chloroflexi*, *Nitrospirae* and *Verrucomicrobia* decreased following biochar additions, while *Actinobacteria*, *Proteobacteria*, *Planctomycetes*, *Bacteroidetes*, *Firmicutes*, and *Gemmatimonadetes* increased, which were dependent on the type and dosage of BC used. Wu et al. (2019) added various BC to oxyfluorfen contaminant soils and investigated the adsorption, degradation, and bioavailability of oxyfluorfen. After introducing 2% BC, the sorption constant was increased by 2.0–3.2 times compared with that of the control soil. Moreover, the degradation in BC-treated soil was faster than that of untreated soil, and the bioavailability of oxyfluorfen was significantly reduced (18–63%). Moreover, the adsorption capacity of biochar amended soil after six months of aging was still 1.5- to 2.5-fold greater compared with that of unamended soil.

5.4.2 Removal of pesticide contaminants by biochar-based composite materials

It is well known that the pores and surfaces of pristine BC are stacked with tar-like sediments which can cover the organic groups and hinder the reaction of BC with contaminations. BC-based composites can maximize the advantages of the pristine BC and other substances. Recently, Taha et al. (2014) used rice straw as biomass and then treated it with phosphoric acid to obtain TBC for removing pesticides in water. Surprisingly, the residual concentration of pesticides was less than the maximum allowed concentration in drinking water (0.1 µg/L) within 10 min. Moreover, all pesticides (except oxamyl) could be removed within 2 h at pH 7.0. The increasing aromaticity of TBC by phosphoric acid treatment can enhance hydrophobic interactions and π-π interactions, which contributed to increase adsorption coefficient (Zhu and Pignatello 2005). Furthermore, Tan et al. (2016) revealed the adsorption capacities of atrazine by BC, Na$_2$S modified BC (BS), and KOH modified BC (BK) were 1.94 mg/g, 2.69 mg/g, and 2.84 mg/g, respectively. The H/C ratios of BS and BK were relatively low, which meant that modified BC was rich in aromatic structure. The more aromatic structures and polyaromatic surfaces can provide more π–π electrons donor–acceptor interaction sites. The π–π electron donor–acceptor interaction between the π-electron-rich (BK/BS) and π-electron-deficient molecule (atrazine) can be

generated by the attraction between opposing quadrupoles and improves the removal rate.

6 New strategies of biochar-based materials

6.1 Immobilized microorganisms on biochar

It is well known that bioremediation is one of the most economical, versatile, and environmentally friendly technology to eliminate pollutants with many advantages. However, the microorganisms have low efficiency in removing high-concentration contaminants and compete with the indigenous microorganisms (Barathi and Vasudevan 2003). Immobilization has been proposed as an effective method to overcome such obstacles, and many researchers have applied BC as a carrier for enhancing microbial degradation. Generally, BC as an ideal carrier material meet the following characteristics: it was readily accessible, low cost, with a porous structure, good biocompatibility, meanwhile facilitating the growth microorganisms. The mechanisms of immobilization of microbial cells to BC include attachment or adsorption on a solid surface, encapsulated within a porous matrix and aggregation by flocculation and crosslinking (Partovinia and Rasekh 2018).

Sodium alginate is commonly used to immobilize microbial cells owing to its simple and relatively mild immobilization procedure. A recent study from Pino et al. (2016) examined the free microbial cells and immobilized microbial cells (on BC and alginate) to enhance phytoremediation of contaminants in the soil. After 60 days of plant growth, the removal of the PCB congener by BC-immobilized microorganisms was up to 30.3%, which was more effective than alginate-immobilized cells (6.8%) and free cells (< 5%). Fresh plant residues were widely used as conventional carriers because they have a high affinity to microorganisms. In another study, Chen et al. (2012) have examined the free microbial cells and immobilized microbial cells (on BC and fresh plant residues) to enhance phytoremediation of polycyclic aromatic hydrocarbons (PAHs) contaminants in the water. The removal percentages of phenanthrene and pyrene from water in immobilized bacteria with plant residues were 85–93% and 94–98%, which were lower than immobilized bacteria with BC (92–100% for phenanthrene and 96–100% for pyrene), and it can be ascribed to the high affinity of BC to PAHs. Phosphate-solubilizing bacteria (PSB) showed both phosphate-solubilizing and Pb-immobilizing capability. However, it cannot multiply rapidly when it is applied in soil for direct competition with indigenous microorganisms. Zhang et al. (2017b) immobilized PSB on cow dung BC to promote the growth and reproduction of PSB, enhance dissolution of phosphorus and immobilization of Pb.

6.2 Biochar-based biofilters

Biofiltration (BF) is a clean technology widely used to treat a variety of contaminants because the secondary waste streams are not produced, economical, and readily available (Mudliar et al. 2010). The biofilter is a solid surface supporting the growth of plants and contaminant-degrading organisms; moreover, the efficiency of biofiltration is highly dependent on it. Generally, as a desirable BF bed medium for a biofiltration system, it meets the following merits: ready availability, durability, economical efficiency, relative stability, and high efficiency for contaminant removal. BC not only meets the requirements above all but also facilitates the growth of plants and microorganisms (Mohanty et al. 2018).

The study confirmed that the application of a biofiltration bed containing BC can serve as a carbon source, which not only enhanced the efficiency of biological treatment systems but also enhanced the removal rate of contaminations. Baltrénas et al. (2016) examined the removal of xylene with birch wood BC-based filtration bed and the maximum removal efficiency reached 86%. BC effectively promoted the growth and reproduction of microorganisms, and the colony-forming units reached 10^7–10^9 CFU/g for fungi, 10^7–10^{10} CFU/g for yeast, and 10^8–10^{10} CFU/g for bacteria, respectively. So inoculated bacteria can play a vital role in BC-based biofilter for the removal of acetone, xylene, and ammonia from the air. Furthermore, BC has the large specific surface area, rich in porous structures, and many surface functional groups on it, the introduction of BC to the biofiltration system can effectively enhance the removal rate of contaminants eliminate through different mechanisms. Deepa et al. (2019) chose BC as principal materials for biofilter bed medium to remove Cr(VI), and the maximum removal rate of Cr(VI) reached 99.99%. The hydroxyl, carboxyl, and carbonyl groups of BC can participate in the removal of Cr(VI) by releasing negatively charged ions such as carbonates and hydroxides, which can precipitate heavy metal ions. Moreover, BC is an electrical conductor, exhibiting a large number of electro active functional groups, revealed itself as the most efficient and sustainable biocompatible material for promoting microbial extracellular electron transfer. Prado et al. (2019) used BC as bed material for constructing biofilters for wastewater treatment. The maximum removal efficiency and degradation rate reached 92% and 185 g-COD m^3/day, respectively. The higher biodegradation efficiency can be attributed to the electroconductivity which is 6.6-fold higher than inert gravel. More importantly, the application of BC requires emission limits while other materials exceeded emission limits.

6.3 Biochar-based 2D membrane

Recently, BC as a new potential absorbent has been widely applied in contaminants' control and water purification because of the high surface area, porosity, and abundant functional groups. However, the applications are still limited due to the low density and small particle size of BC, so it is not easy to separate BC from water. Mixed matrix membrane (MMM) included continuous polymer phase (such as glassy, rubbery) and was evenly dispersed with filler particle (Dechnik et al. 2017). In order to address these issues, great efforts have been made to combine the BC with polymeric matrix to develop a new class of membranes, called BC-based 2D membrane. Recently, MMM has been widely used in wastewater treatment because of its superior removal efficiency for contaminants. Moreover, BC is easier to assemble into a 2D membrane through mutual interactions compared with other types of adsorbents (Xie et al. 2015). Incorporating BC into matrix membrane is a promising strategy that can not only enhance the adsorption capacity and reduce the cost but also overcome the above limitations of the BC.

The BC-based 2D membrane could be easily composed of BC and polymer via casting and electrospinning processes. He et al. (2017) prepared a BC-based membrane by embedding BC particles into polysulfone (PSF) via casting for the treatment of wastewater contaminated by copper and lead. The BC-based membrane is more hydrophilic and has higher water flux than the pure PSF membrane. The maximum adsorption capacities reached 90.36% and 90.16% for copper and lead, respectively. After four cycles, the adsorption capacity could still reach 87.4% for copper, and 86.83% for lead, respectively. It is demonstrated that embedding BC particles into PSF cannot block the adsorption sites of BC. Currently, polyvinylidene fluoride (PVDF) is another popular polymer in BC-based membranes; other studies blended BC with PVDF to construct BC-based membrane. Ghaffar et al. (2018) composed a BC-based membrane by casting the mixture of BC and PVDF, and the resultant membrane displayed a high mechanical strength and porous structures with evenly dispersed BC particles on the surface and cross-section of the membrane. And the resultant membrane exhibited an amazing adsorption capacity to Rhodamine B dye (RhB) (187 mg/g). Furthermore, the resultant membranes can be effectively recovered from water, which shows a promising potential for applications in environmental remediation.

6.4 3D biochar-based macrostructures

Generally, the bulk of BC ranges from millimeter to centimeter, small BC particles limit the application in water treatment, and the BC-based membrane can solve the limitation of BC materials in recycle and secondary pollution.

However, BC has numerous extraordinary properties and it is necessary to extend the application in broader practical and fields. 3D BC-based macrostructure is a hierarchical porous-structured carbonaceous hydrogel or aerogel as a novel method for BC application.

Aerogel and hydrogels are two typical parts of gels that are classified by encompassing medium (water or air) (Liang et al. 2012). Conventional aerogels lack mechanical stability and are of high-cost on a large scale because of the limitations of industrial supercritical drying. Luckily, this fatal disadvantage could be eliminated by coating polymer on 3D networks. For example, Wang et al. (2016b) synthesized the carbonaceous aerogel from biomass and modified it with polydimethylsiloxane (PDMS) and obtained an excellent performance in separating and collecting oil and organic solvent from water. Moreover, this carbonaceous aerogel is small and portable and could be used in emergencies such as organic solvent leakage and tanker spills. Currently, a new class of carbonaceous hydrogel was synthesized by the one-step method using hydrothermal carbonization (HTC). This method is a template-directed carbonization-activation method that has significant advantages, such as easy and precise control of the structural parameters and mechanical strength, extraordinary flexibility, and high chemical reactivity. Liu et al. (2019a) used the one-step direct carbonization-activation method to synthesize the 3D porous BC aerogel exhibiting high porosity and high surface area (2607 m^2/g). Moreover, the removal rate of phenicol antibiotics (PABs) reached 90% within 10 min by 3D porous BC aerogel via pore-filling effect, π–π/n–π EDA interaction, and electrostatic interaction. Furthermore, Zhang et al. (2017a) prepared carbonaceous hydrogel using waste soybean dreg, and carbonaceous hydrogel displayed a high and fast adsorption capacity for Zn(II), Fe(III), Cu(II), and Cr(III), which was 121.2, 78.5, 75.4 and 41.7 mg g^{-1}, respectively. In the first two minutes, the removal rate reached 88. 6, 81.9, 84.4, and 75.1% of the amount of equilibrium adsorption, respectively.

To summarize, 3D BC-based macrostructure exhibited excellent performances for removing organic pollutants and heavy metal because of high adsorption capacity, recycling performance, and porous structure. Apart from this, 3D BC-based macrostructure is widely applied in energy storage and electrochemical catalysis reactions.

## 7 Potential risks of biochar and biochar-based composite materials

A large number of toxic substances such as PAHs, dioxin (PCDD and PCDF), and acrolein were formed during the preparation of BC (El-Naggar et al. 2019a; Zheng et al. 2019). Different preparation conditions not only affect the physicochemical properties of BC, but also affect the

biological toxicity of BC. According to the literature, the concentrations of PAH in BC were affected by the pyrolysis temperature and biomass (Keiluweit et al. 2012). Lyu et al. (2016) and Hale et al. (2012) have demonstrated that the BC prepared at low temperature exhibited higher biological toxicity. The concentrations of PAH in BC was positively correlated with the pyrolysis temperature. The concentration was 8.6×10^2 µg/kg and reached the maximum at 400 °C, then decreased with the temperature increased and dropped to the minimum of 5.9×10^2 µg/kg at 700 °C. The concentration of PAH in ordinary BC was 0.07–4 µg/g, and reached 17–27 µg/g when prepared from paper mill sludge and wood, which was much higher than the ordinary value (Devi and Saroha 2014b; Keiluweit et al. 2012). PCDD and PCDF are highly toxic compounds, whose concentrations were 610 pg/g and 67 pg/g at 300 °C and 700 °C, respectively. Concentrations of PCDD and PCDF at 700 °C were much lower than that at temperature of 300 °C (Lyu et al. 2016). Besides, the toxicity of BC is related to particle size and dosage. Sigmund et al. (2017) have shown that BC has toxic effects on fibroblasts and the toxicity of BC is related to the particle properties and size of BC. Zhang et al. (2019c) suggested that 1 and 3% BC amend soil could effectively reduce the toxicity of mesotrione to earthworms. However, 10% BC amended soil significantly inhibitted the growth of earthworm though the DNA damaged. Furthermore, pristine BC materials contain potentially toxic elements such as heavy metals, metalloids. The content of heavy metals in BC varied with the biomass. For example, compared with green waste, BC made from sludge and animal manure was rich in heavy metals such as Pb, Cd, Cu, Mn, Zn, Ni, and Cr, which limited the application of BC (Zheng et al. 2019). In addition, long-term application of BC may release internal toxic substances via aging and debilitating processes, which can arouse secondary pollution in water environments. Therefore, the potential hazards should be considered in the preparation and application of BC to reduce the harm to the environment. Moreover, BC can effectively remove water pollutants remaining in the primary stage of the experiment. Short-term simulation studies cannot ensure that long-term applications in water treatment are risk-free. Therefore, long-term water experiments and risk assessment are essential for BC applications in water or soil treatment.

BC not only releases toxic substances, but also may show side effects on organisms (Lian et al. 2017). As known to all, the pH range of BC is from slightly acidic to alkaline and increases with the increase of pyrolysis temperature (Kookana et al. 2011; Al-wabel et al. 2013). The addition of BC to the soil will affect the acidity and alkalinity, thereby affecting the utilization of toxic substances by microorganisms (Kookana et al. 2011). Gomez-Eyles et al. (2011) suggested that during the exposure to BC, the accumulation of pollutants and the weight of earthworms were significantly reduced. Likewise, BC has strong adsorption of pesticides, which will decrease the bioavailability and efficiency in the soil (Kookana 2010; Jonker et al. 2004). Furthermore, BC can generate free radicals, which will cause germination inhibition, growth retardation, and plasma membrane damage (Liao et al. 2014). And ROS generated by free radicals may cause oxidative stress and induce cellular toxicity (Xia

Fig. 5 The graphical abstract of this review
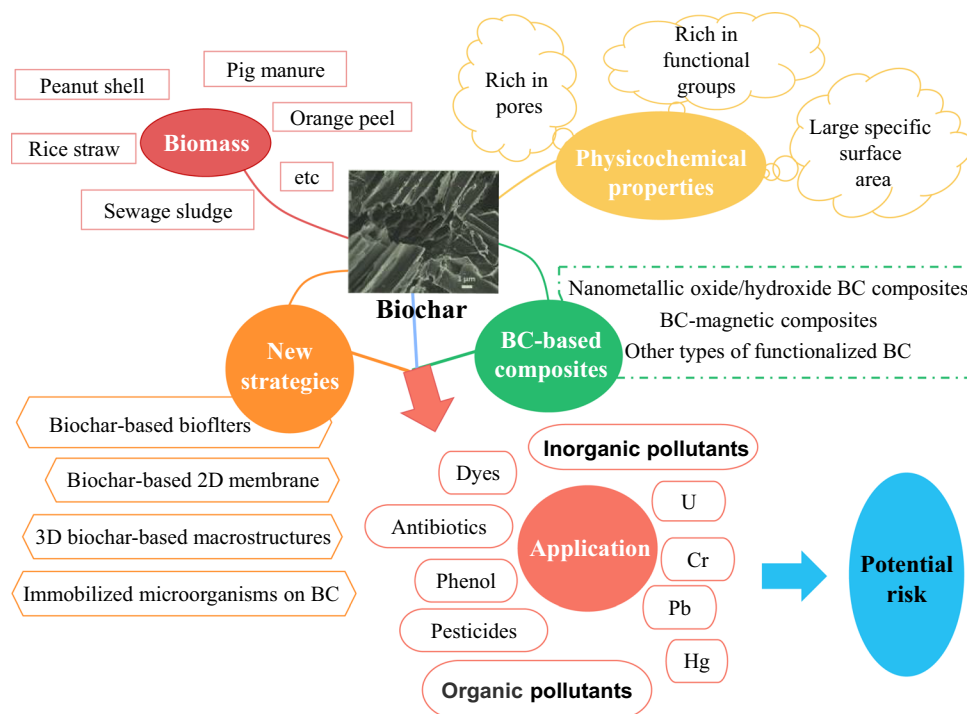
et al. 2006; Cheng et al. 2018). In addition, Spokas et al. (2012) reported that approximately 20% of studies showed that BC incorporation exhibited a negative impact on yield or growth.

Apart from BC, the potential risk of modification materials cannot be overlooked. For example, Adams et al. (2006) showed that TiO_2, ZnO, and SiO_2 were all toxic to microorganisms. Azargohar and Dalai (2008) have shown that BC was toxic to *D. magna* after steam activation. Similarly, Wahab et al. (2013) reported that the melanoma cancer cells produced reactive oxygen species (ROS) and apoptosis after contact with nZnO. These materials may leach out after several times of reuse and were harmful to the environment (Huang et al. 2019). Furthermore, the preparation of some composite materials may introduce KOH, NaOH, HCl, and H_2SO_4, which will change the pH value of BC, thereby changing the soil or water environment, and affecting the growth and reproduction of organisms (Kookana et al. 2011). BC-based composites can effectively improve the removal efficiency of contaminants, but there were relatively few studies on stability and biological toxicity. Therefore, it was necessary to comprehensively evaluated the stability and biological effects of the BC-based composites in water/soil environments before the practical applications so as to avoid the toxic substances shedding from the composites that caused secondary environmental contaminant and biological damaged.

8 Conclusion and prospective

This article reviewed the latest developments of BC and BC-based composite materials and summarized some new strategies of BC-based materials by emphasizing the preparation methods, the physicochemistry properties, the pollution removal performance, and adsorption mechanisms. The graphical abstract of this review is summarized in Fig. 5. Moreover, the potential risks of BC and BC-based composites to the environment were also reviewed. In brief, more attention should be paid to practical applications and more studies should be provided to solve the existing problems. For example, (1) current studies are lacking in studying the stability of BC or BC-based composites and their biological toxicity to aquatic and soil microorganisms; (2) short of field trials, most of studies are conducted in laboratories, and the conclusion of a perfect simulation is not suitable in field trials; (3) the mechanism of BC removal of contaminants is still inconclusive, and the relationships between biomass, preparation methods, and properties are still unclear enough; (4) the preparation of ideal BC needs to avoid unnecessary contaminants in the preparation process.

Declarations

References

Abdul G, Zhu XY, Chen BL (2017) Structural characteristics of biochar-graphene nanosheet composites and their adsorption performance for phthalic acid esters. Chem Eng J 319:9–20

Adams LK, Lyon DY, Alvarez PJJ (2006) Comparative eco-toxicity of nanoscale TiO_2, SiO_2, and ZnO water suspensions. Water Res 40(19):3527–3532

Ahmad M, Lee SS, Dou XM, Mohan D, Sung JK, Yang JE, Ok YS (2012) Effects of pyrolysis temperature on soybean stover- and peanut shell-derived biochar properties and TCE adsorption in water. Biores Technol 118:536–544

Ali N, Khan S, Yao HY, Wang J (2019) Biochars reduced the bioaccessibility and (bio)uptake of organochlorine pesticides and changed the microbial community dynamics in agricultural soils. Chemosphere 224:805–815

Al-Wabel MI, Al-Omran A, El-Naggar AH, Nadeem M, Usman A (2013) Pyrolysis temperature induced changes in characteristics and chemical composition of biochar produced from conocarpus wastes. Biores Technol 131:374–379

Andrew A, Vivekanandhan S, Rodriguez-Uribe A, Misra M, Mohanty AM (2016) Oxidative acid treatment and characterization of new biocarbon from sustainable Miscanthus biomass. Sci Total Environ 550:241–247

Angin D (2013) Effect of pyrolysis temperature and heating rate on biochar obtained from pyrolysis of safflower seed press cake. Biores Technol 128:593–597

Azargohar R, Dalai AK (2008) Steam and KOH activation of biochar: experimental and modeling studies. Microporous Mesoporous Mater 110:413–421

Baltrėnas P, Baltrėnaitė E, Kleiza J, Švedienė J (2016) A biochar-based medium in the biofiltration system: Removal efficiency, microorganism propagation, and the medium penetration modeling. J Air Waste Manag Assoc 66(7):673–686

Banat FA, Al-Bashir B, Al-Asheh S, Hayajneh O (2000) Adsorption of phenol by bentonite. Environ Pollut 107(3):391–398

Barathi S, Vasudevan N (2003) Bioremediation of crude oil contaminated soil by bioaugmentation of Pseudomonas fluorescens

NS1. J Environ Sci Health Part A Toxic/hazard Subst Environ Eng 38:1857–1866

Bender J, Lee RF, Phillips P (1995) Uptake and transformation of metals and metalloids by microbial mats and their use in bioremediation. J Ind Microbiol Biotechnol 14:113–118

Braadbaart F, Poole I (2008) Morphological, chemical and physical changes during charcoalification of wood and its relevance to archaeological contexts. J Archaeol Sci 35(9):2434–2445

Cao XD, Harris W (2010) Properties of dairy-manure-derived biochar pertinent to its potential use in remediation. Biores Technol 101(14):5222–5228

Cao XD, Ma L, Gao B, Harris W (2008) Dairy-Manure Derived Biochar Effectively Sorbs Lead and Atrazine. Environ Sci Technol 43(9):3285–3291

Cha JS, Park SH, Jung SC (2016) Production and Utilization of Biochar: A Review. J Ind Eng Chem 40:1–15

Chakraborty P, Banerjee S, Kumar S, Sadhukhan S, Halder G (2018) Elucidation of ibuprofen uptake capability of raw and steam activated biochar of Aegle marmelos shell: Isotherm, Kinetics, Thermodynamics and Cost estimation. Process Saf Environ Prot 118:10–23

Chaukura N, Murimba EC, Gwenzi W (2017) Synthesis, characterisation and methyl orange adsorption capacity of ferric oxide-biochar nano-composites derived from pulp and paper sludge. Appl Water Sci 7(5):2175–2186

Chen BL, Chen ZM (2009) Sorption of naphthalene and 1-naphthol by biochars of orange peels with different pyrolytic temperatures. Chemosphere 76(1):127–133

Chen BL, Chen ZM, Lv SF (2011) A novel magnetic biochar efficiently sorbs organic pollutants and phosphate. Biores Technol 102(2):716–723

Chen BL, Yuan MX, Qian LB (2012) Enhanced bioremediation of PAH-contaminated soil by immobilized bacteria with plant residue and biochar as carriers. J Soils Sediments 12:1350–1359

Chen T, Zhang YX, Wang HT, Lu WJ, Zhou ZY, Zhang YC, Ren LL (2014) Influence of pyrolysis temperature on characteristics and heavy metal adsorptive performance of biochar derived from municipal sewage sludge. Biores Technol 164:47–54

Cheng YJ, Dong HR, Lu Y, Hou KJ, Wang YY, Ning Q, Li L, Wang B, Zhang LH, Zeng GM (2018) Toxicity of sulfide-modified nanoscale zero-valent iron to *Escherichia* coli in aqueous solutions. Chemosphere 220:523–530

Choi YK, Kan E (2019) Effects of pyrolysis temperature on the physicochemical properties of alfalfa-derived biochar for the adsorption of bisphenol A and sulfamethoxazole in water. Chemosphere 218:741–748

Cope CO, Webster DS, Sabatini DA (2014) Arsenate adsorption onto iron oxide amended rice husk char. Sci Total Environ 488–489:554–561

Cross A, Sohi SP (2013) A method for screening the relative long-term stability of biochar. Global Change Biology Bioenergy 5(2):215–220

Dawood S, Sen TK, Phan C (2016) Adsorption removal of Methylene Blue (MB) dye from aqueous solution by bio-char prepared from Eucalyptus sheathiana bark: kinetic, equilibrium, mechanism, thermodynamic and process design. Desalin Water Treat 57(59):28964–28980

Dechnik J, Gascon J, Doonan CJ, Janiak C, Sumby C (2017) Mixed matrix membranes. Angew Chem 56(32):9292–9310

Deepa A, Prakash P, Mishra BK (2019) Performance of biochar-based filtration bed for the removal of Cr(VI) from pre-treated synthetic tannery wastewater. Enviro Technol 42(2):257–269

Deng XY, Luan QX, Chen WT, Wang YL, Wu MH, Zhang HJ, Jiao Z (2009) Nanosized zinc oxide particles induce neural stem cell apoptosis. Nanotechnology 20:115101

Deng YY, Huang S, Laird DA, Wang XG, Dong CQ (2018) Quantitative mechanisms of cadmium adsorption on rice straw- and swine manure-derived biochars. Environ Sci Pollut Res 25(32):32418–32432

Devi P, Saroha AK (2014a) Synthesis of the magnetic biochar composites for use as an adsorbent for the removal of pentachlorophenol from the effluent. Biores Technol 169:525–531

Devi P, Saroha AK (2014b) Risk analysis of pyrolyzed biochar made from paper mill effluent treatment plant sludge for bioavailability and eco-toxicity of heavy metals. Biores Technol 162:308–315

Dong XL, Ma LQ, Li YC (2011) Characteristics and mechanisms of hexavalent chromium removal by biochar from sugar beet tailing. J Hazard Mater 190(1–3):909–915

Dong HR, Deng JM, Xie YK, Zhao ZC, J, Cheng Y J, Zeng G M, (2017) Stabilization of nanoscale zero-valent iron (nZVI) with modified biochar for Cr(VI) removal from aqueous solution. J Hazard Mater 332:79–86

El-Naggar A, Shaheen SM, Ok YS, Rinklebe J (2018) Biochar affects the dissolved and colloidal concentrations of Cd, Cu, Ni, and Zn and their phytoavailability and potential mobility in a mining soil under dynamic redox-conditions. Sci Total Environ 624:1059–1071

El-Naggar A, El-Naggar AH, Shaheen SM, Sarkar B, Chang SX, Tsang DCW, Rinklebe J, Ok YS (2019a) Biochar composition-dependent impacts on soil nutrient release, carbon mineralization, and potential environmental risk: a review. J Environ Manage 241:458–467

El-Naggar A, Lee MH, Hur J, Lee HY, Igalavithana AD, Shaheen SM, Ryu C, Rinklebe J, Tsang DCW, Ok YS (2019b) Biochar-induced metal immobilization and soil biogeochemical process: an integrated mechanistic approach. Sci Total Environ 698:134112

El-Naggar A, Shaheen SM, Hseu ZY, Wang SL, Ok YS, Rinklebe J (2019c) Release dynamics of As Co, and Mo in a biochar treated soil under pre-definite redox conditions. Sci Total Environ 657:686–695

Essandoh M, Kunwar B, Pittman CU, Mohan D, Mlsna T (2015) Sorptive removal of salicylic acid and ibuprofen from aqueous solutions using pine wood fast pyrolysis biochar. Chem Eng J 265:219–227

Faheem YuHX, Liu J, Shen JY, Sun XY, Li JS, Wang LJ (2016) Preparation of MnOx-loaded biochar for Pb^{2+} removal: Adsorption performance and possible mechanism. J Taiwan Inst Chem Eng 00:1–8

Fan SS, Wang Y, Wang Z, Tang J, Li XD (2017) Removal of methylene blue from aqueous solution by sewage sludge-derived biochar: adsorption kinetics, equilibrium, thermodynamics and mechanism. J Environ Chem Eng 5(1):601–611

Fan SS, Wang Y, Li Y, Wang Z, Xie ZX, Tang J (2018) Removal of tetracycline from aqueous solution by biochar derived from rice straw. Environ Sci Pollut Res 25(29):29529–29540

Fan J, Chen X, Xu ZB, Xu XY, Zhao L, Qiu H, Cao XD (2020) One-pot synthesis of nZVI-embedded biochar for remediation of two mining arsenic-contaminated soils: Arsenic immobilization associated with iron transformation - ScienceDirect. J Hazard Mater 398:122901

Funke A, Ziegler F (2010) Hydrothermal carbonization of biomass: A summary and discussion of chemical mechanisms for process engineering. Biofuels, Bioprod Biorefin 4(2):160–177

Gao RL, Hu HQ, Fu Q, l, Li Z H, Xing Z Q, Ali U, Zhu J, Liu Y H, (2020) Remediation of Pb, Cd, and Cu contaminated soil by co-pyrolysis biochar derived from rape straw and orthophosphate: Speciation transformation, risk evaluation and mechanism inquiry. Sci Total Environ 730:139119

Gascó G, Paz-Ferreiro J, Álvarez ML, Saa A, Méndez A (2018) Biochars and hydrochars prepared by pyrolysis and hydrothermal carbonisation of pig manure. Waste Manage 79:395–403

Ghaffar A, Zhu XY, Chen B (2018) Biochar composite membrane for high performance pollutant management: Fabrication, structural characteristics and synergistic mechanisms. Environ Pollut 233:1013–1023

Gholami P, Dinpazhoh L, Khataee A, Orooji Y (2019) Sonocatalytic activity of biochar-supported ZnO nanorods in degradation of gemifloxacin: synergy study, effect of parameters and phytotoxicity evaluation. Ultrason Sonochem 55:44–56

Gomez-Eyles JL, Sizmur T, Collins CD, Hodson E (2011) Effects of biochar and the earthworm Eisenia fetida on the bioavailability of polycyclic aromatic hydrocarbons and potentially toxic elements. Environ Pollut 159(2):616–622

Hairuddin MN, Mubarak NM, Khalid M, Abdullah EC, Walvekar R, Karri RR (2019) Magnetic palm kernel biochar potential route for phenol removal from wastewater. Environ Sci Pollut Res 26(34):35183–35197

Hale SE, Lehmann J, Rutherford D, Zimmerman AR, Bachmann RT, Shitumbanuma V, O'Toole A, Sundqvist KL, Cornelissen G (2012) Quantifying the total and bioavailable polycyclic aromatic hydrocarbons and dioxins in biochars. Environ Sci Technol 46(5):2830–2838

Han YT, Cao X, Ouyang X, Sohi SP, Chen JW (2016) Adsorption kinetics of magnetic biochar derived from peanut hull on removal of Cr (VI) from aqueous solution: effects of production conditions and particle size. Chemosphere 145:336–341

Hao MJ, Qiu MQ, Yang H, Hu BW, Wang XX (2021) Recent advances on preparation and environmental applications of MOF-derived carbons in catalysis. Sci Total Environ 760:143333

He JS, Song YH, Chen JP (2017) Development of a novel biochar/PSF mixed matrix membrane and study of key parameters in treatment of copper and lead contaminated water. Chemosphere 186:1033–1045

Heilmann SM, Davis HT, Jader LR, Lefebvre PA, Sadowsky MJ, Schendel FJ, Keitz MJ, Valentas KJ (2010) Hydrothermal carbonization of microalgae. Biomass Bioenerg 34(6):875–882

Houde M, Muir DCG, Kidd KA, Guildford S, Drouillard K, Evans MS, Wang XW, Whittle DM, Haffner D, Kling D (2008) Influence of lake characteristics on the biomagnification of persistent organic pollutants in lake trout food webs. Environ Toxicol Chem 27(10):2169–2178

Hu BW, Ai YJ, Jin J, Hayat T, Alsaedi A, Zhuang L, Wang XK (2020) Efficient elimination of organic and inorganic pollutants by biochar and biochar-based materials. Biochar 2:47–64

Huang DL, Wang X, Zhang C, Zeng GM, Peng ZW, Zhou J, Cheng M, Wang RZ, Hu ZX, Qin X (2017) Sorptive removal of ionizable antibiotic sulfamethazine from aqueous solution by graphene oxide-coated biochar nanocomposites: Influencing factors and mechanism. Chemosphere 186:414–421

Huang Q, Song S, Chen Z, Hu BW, Chen JR, Wang XK (2019) Biochar-based materials and their applications in removal of organic contaminants from wastewater: state-of-the-art review. Biochar 1:45–73

Huggins TM, Haeger A, Biffinger JC, Ren ZYJ (2016) Granular biochar compared with activated carbon for wastewater treatment and resource recovery. Water Res 94:225–232

Inyang MI, Gao B, Yao Y, Xue YW, Zimmerman A, Mosa A, Pullammanappallil P, Cao XD (2016) A Review of Biochar as a Low-Cost Adsorbent for Aqueous Heavy Metal Removal. Crit Rev Environ Sci Technol 46(4):406–433

Ioannou K, Hadjiyiannis P, Liatsou I, Pashalidis I (2019) U(VI) adsorption by biochar fiber–MnO$_2$ composites. J Radioanal Nucl Chem 320:425–432

Islam MS, Ahmed MK, Raknuzzaman M, Islam MK (2015) Heavy metal pollution in surface water and sediment: A preliminary assessment of an urban river in a developing country. Ecol Ind 48:282–291

Jin HM, Capareda S, Chang ZZ, Gao J, Xu YD, Zhang JY (2014) Biochar pyrolytically produced from municipal solid wastes for aqueous As(V) removal: adsorption property and its improvement with KOH activation. Biores Technol 169:622–629

Jonker MTO, Hoenderboom AM, Koelmans AA (2004) Effects of sedimentary sootlike materials on bioaccumulation and sorption of polychlorinated biphenyls. Environ Toxicol Chem 23(11):2563–2570

Jung KW, Lee SY, Lee YJ (2018) Facile one-pot hydrothermal synthesis of cubic spinel-type manganese ferrite/biochar composites for environmental remediation of heavy metals from aqueous solutions. Biores Technol 261:1–9

Kochermann J, Gorsch J, Wirth B, Muhlenberg J, Klemm M (2018) Hydrothermal carbonization: Temperature influence on hydrochar and aqueous phase composition during process water recirculation. J Environ Chem Eng 6(4):5481–5487

Keiluweit M, Kleber M, Sparrow MA, Simoneit BRT, Prahl FG (2012) Solvent-extractable polycyclic aromatic hydrocarbons in biochar: influence of pyrolysis temperature and feedstock. Environ Sci Technol 46(17):9333–9341

Khataee A, Kayan B, Gholami P, Kalderis D, Akay S (2017) Sonocatalytic degradation of an anthraquinone dye using TiO$_2$-biochar nanocomposite. Ultrason Sonochem 39:120–128

Khataee A, Gholami P, Kalderis D, Pachatouridou E, Konsolakis M (2018) Preparation of novel CeO$_2$-biochar nanocomposite for sonocatalytic degradation of a textile dye. Ultrason Sonochem 41:503–513

Komkiene J, Baltrenaite E (2016) Biochar as adsorbent for removal of heavy metal ions [Cadmium(II), Copper(II), Lead(II), Zinc(II)] from aqueous phase. Int J Environ Sci Technol 13(2):471–482

Kookana RS (2010) The role of biochar in modifying the environmental fate, bioavailability, and efficacy of pesticides in soils: a review. Aust J Soil Res 48:627–637

Kookana RS, Sarmah AK, Zwieten LV, Krull E, Singh B (2011) Biochar application to soil: agronomic and environmental benefits and unintended consequences. Adv Agron 112:103–143

Kumar S, Loganathan VA, Gupta RB, Barnett MO (2011) An assessment of U(VI) removal from groundwater using biochar produced from hydrothermal carbonization. J Environ Manage 92(10):2504–2512

Lawal AA, Hassan MA, Farid MAA, Anuar TATY, Samsudin MH, Yusoff MZM, Zakaria MR, Mokhtar MN, Shirai Y (2021) Adsorption mechanism and effectiveness of phenol and tannic acid removal by biochar produced from oil palm frond using steam pyrolysis. Environ Pollut 269:116197

Lawrinenko M, Jing D, Banik C, Laird DA (2017) Aluminum and iron biomass pretreatment impacts on biochar anion exchange capacity. Carbon 118:422–430

Lee JW, Kidder M, Evans BR, Paik S, Buchanan AC III, Garten CT, Brown RC (2010) Characterization of biochars produced from cornstovers for soil amendment. Environ Sci Technol 44(20):7970–7974

Lee CG, Hong SH, Hong SG (2019) Production of biochar from food waste and its application for phenol removal from aqueous solution. Water Air Soil Pollut 230(3):70

Lehmann J, Rillig MC, Thies J, Masiello CA, Hockaday WC, Crowley D (2011) Biochar effects on soil biota—a review. Soil Biol Biochem 43(9):1812–1836

Leng LJ, Huang HJ (2018) An overview of the effect of pyrolysis process parameters on biochar stability. Biores Technol 270:627–642

Li A, Liu HL, Wang H, Xu HB, Jin LF, Liu JL, Hu JH (2016) Effects of Temperature and Heating Rate on the Characteristics of Molded Bio-char. BioResources 11(2):3259–3274

Li HB, Dong XL, Silva EB, Oliveira LM, Chen YS, Ma LQ (2017a) Mechanisms of metal sorption by biochars: Biochar characteristics and modifications. Chemos Environ Toxicol Risk Assess 178:466–478

Li H, Qiu YF, Wang XL, Yang J, Yu YJ, Chen YQ (2017b) Biochar supported Ni/Fe bimetallic nanoparticles to remove 1,1,1-trichloroethane under various reaction conditions. Chemosphere 169:534–541

Li CJ, Zhang L, Gao Y, Li AM (2018a) Facile synthesis of nano ZnO/ZnS modified biochar by directly pyrolyzing of zinc contaminated corn stover for Pb(II), Cu(II) and Cr(VI) removals. Waste Manage 79:625–637

Li L, Wang YY, Xu JT, Floar JRV, Hoque S, Berge ND (2018b) Quantifying the sensitivity of feedstock properties and process conditions on hydrochar yield, carbon content, and energy content. Biores Technol 262:284–293

Li MX, Li HB, Chen TH, Dong C, Sun YB (2018c) Synthesis of magnetic biochar composites for enhanced uranium(VI) adsorption. Sci Total Environ 651:1020–1028

Li RH, Deng HX, Zhang XF, Wang JJ, Awasthi MK, Wang Q, Xiao R, Zhou BY, Du J, Zhang ZQ (2018d) High-efficiency removal of Pb(II) and humate by a CeO_2–MoS_2 hybrid magnetic biochar. Biores Technol 273:335–340

Li L, Yang M, Lu Q, Zhu WK, Ma HQ, Dai LC (2019a) Oxygen-rich biochar from torrefaction: A versatile adsorbent for water pollution control–Science Direct. Biores Technol 294:122142

Li N, Yin ML, Tsang DCW, Yang ST, Liu J, Li X, Song G, Wang J (2019b) Mechanisms of U(VI) removal by biochar derived from *Ficus microcarpa* aerial root: A comparison between raw and modified biochar. Sci Total Environ 697:134115

Lian F, Xing BS (2017) Black carbon (biochar) in water/soil environments: molecular structure, sorption, stability, and potential risk. Environ Science Technol 51(23):13517–13532

Liang HW, Guan QF, Chen LF, Zhu Z, Yu SH (2012) Macroscopic-scale template synthesis of robust carbonaceous nanofiber hydrogels and aerogels and their applications. Angew Chem Int Ed 124(21):5191–5195

Liang J, Li XM, Yu ZG, Zeng GM, Luo Y, Jiang LB, Yang ZX, Qian YY, Hu HP (2017) Amorphous MnO_2 modified biochar derived from aerobically composted swine manure for adsorption of Pb(II) and Cd(II). ACS Sustain Chem Eng 5(6):5049–5058

Liao SH, Pan B, Li H, Zhang D, Xing BS (2014) Detecting free radicals in biochars and determining their ability to inhibit the germination and growth of corn, wheat and rice seedlings. Environ Sci Technol 48(15):8581–8587

Lisowski P, Colmenares JC, Mašek O, Lisowski W, Lisovytskiy D, Kamińska A, Łomot D (2017) Dual functionality of TiO_2/biochar hybrid materials: photocatalytic phenol degradation in liquid phase and selective oxidation of methanol in gas phase. ACS Sustain Chem Eng 5(7):6274–6287

Liu Z, Zhang FS (2011) Removal of copper (II) and phenol from aqueous solution using porous carbons derived from hydrothermal chars. Desalination 267(1):101–106

Liu P, Liu WJ, Jiang H, Chen JJ, Li WW, Yu HQ (2012) Modification of bio-char derived from fast pyrolysis of biomass and its application in removal of tetracycline from aqueous solution. Biores Technol 121:235–240

Liu P, Jiang R, Zhou WC, Zhu H, Xiao W, Wang DH, Mao XH (2015) g-C_3N_4 Modified biochar as an adsorptive and photocatalytic material for decontamination of aqueous organic pollutants. Appl Surf Sci 358:231–239

Liu H, Wei YF, Luo JM, Li T, Wang D, Luo SL, Crittenden JC (2019a) 3D hierarchical porous-structured biochar aerogel for rapid and efficient phenicol antibiotics removal from water. Chem Eng J 368:639–648

Liu JL, Zhou BQ, Zhang H, Ma J, Mu B, Zhang WB (2019b) A novel Biochar modified by Chitosan-Fe/S for tetracycline adsorption and studies on site energy distribution. Biores Technol 294:122152

Liu YY, Sohi SP, Liu SY, Guan JJ, Zhou JY, Chen JW (2019c) Adsorption and reductive degradation of Cr(VI) and TCE by a simply synthesized zero valent iron magnetic biochar. J Environ Manage 235:276–281

Liu HY, Song C, Zhao S, Wang SG (2020) Biochar-induced migration of tetracycline and the alteration of microbial community in agricultural soils. Sci Total Environ 706:136086.1-136086.7

Liu XL, Pang HW, Liu XW, Li Q, Zhang N, Mao L, Qiu MQ, Hu BW, Yang H, Wang XK (2021a) Orderly porous covalent organic frameworks-based materials: superior adsorbents for pollutants removal from aqueous solutions. The Innovation 2:100076

Liu XL, Ma R, Zhuang L, Hu BW, Chen JR, Liu XY, Wang XK (2021b) Recent developments of doped g-C_3N_4 photocatalysts for the degradation of organic pollutants. Crit Rev Environ Sci Technol 51:751–790

Lu HL, Zhang WH, Yang YX, Huang XF, Wang SH, Qiu RL (2011) Relative distribution of Pb~(2+) sorption mechanisms by sludge-derived biochar. Water Res 46(3):854–862

Lu HP, Li ZA, Gascó G, Méndez A, Shen Y, Paz-Ferreiro J (2017) Use of magnetic biochars for the immobilization of heavy metals in a multi-contaminated soil. Sci Total Environ 622–623:892–899

Lu LL, Shan R, Shi YY, Wang SX, Yuan HR (2019) A novel TiO_2/biochar composite catalysts for photocatalytic degradation of methyl orange. Chemosphere 222:391–398

Lu L, Yu WT, Wang YF, Zhang K, Zhu XM, Zhang YC, Wu YJ, Ullah H, Xiao X, Chen BL (2020) Application of biochar-based materials in environmental remediation: from multi-level structures to specifc devices. Biochar 2:1–2

Luján LS, Román SV, Toledo C, Parejo OS, Mansour AE, Abad J, Amassian A, Benito AM, Maser WK, Urbina A (2019) Environmental impact of the production of graphene oxide and reduced graphene oxide. SN Appl Sci 1(2):1–12

Luo JW, Li X, Ge CG, Müller K, Yu HM, Huang P, Li JT, Tsang DCW, Bolan NS, Rinklebe J, Wang HL (2018) Sorption of norfloxacin, sulfamerazine and oxytetracycline by KOH-modified biochar under single and ternary systems. Biores Technol 263:385–392

Lyu HH, He YH, Tang JC, Hecker M, Liu QL, Jones PD, Codling G, Giesy JP (2016) Effect of pyrolysis temperature on potential toxicity of biochar if applied to the environment. Environ Pollut 218:1–7

Lyu HH, Gao B, He F, Zimmerman AR, Ding C, Huang H, Tang JC (2018) Effects of ball milling on the physicochemical and sorptive properties of biochar: Experimental observations and governing mechanisms. Environ Pollut 233:54–63

Ma Y, Liu WJ, Zhang N, Li YS, Jiang H, Sheng GP (2014) Polyethylenimine modified biochar adsorbent for hexavalent chromium removal from the aqueous solution. Biores Technol 169:403–408

Mohammed NAS, Abu-Zurayk RA, Hamadneh I, Al-Dujaili AH (2018) Phenol adsorption on biochar prepared from the pine fruit shells: Equilibrium, kinetic and thermodynamics studies. J Environ Manage 226:377–385

Mohan D, Kumar H, Sarswat A, Alexandre-Franco M, Pittman CU (2013) Cadmium and lead remediation using magnetic oak wood and oak bark fast pyrolysis bio-chars. Chem Eng J 236(2):513–528

Mohan D, Singh P, Sarswat A, Steele PH, Pittman CU (2015) Lead sorptive removal using magnetic and nonmagnetic fast pyrolysis energy cane biochars. J Colloid Interface Sci 448:238–250

Mohanty P, Nanda S, Pant KK, Naik S, Kozinski JA, Dalai AK (2013) Evaluation of the physiochemical development of biochars

obtained from pyrolysis of wheat straw, timothy grass and pine-wood: effects of heating rate. J Anal Appl Pyrol 104:485–493

Mohanty SK, Valenca R, Berger AW, Yu IKM, Xiong XN, Saunders TM, Tsang DCW (2018) Plenty of room for carbon on the ground: potential applications of biochar for stormwater treatment. Sci Total Environ 625:1644–1658

Mudliar S, Giri B, Padoley K, Satpute D, Dixit R, Bhatt P, Pandey R, Juwarkar A, Vaidya A (2010) Bioreactors for treatment of VOCs and Odours—a review. J Environ Manage 91(5):1039–1054

Mullen CA, Boateng AA, Goldberg NM, Lima IM, Laird DA, Hicks KB (2010) Bio-oil and bio-char production from corn cobs and stover by fast pyrolysis. Biomass Bioenerg 34(1):67–74

Park JH, Ok YS, Kim SH, Choc JS, Heo JS, Delauned RD, Seoc DC (2015) Evaluation of phosphorus adsorption capacity of sesame straw biochar on aqueous solution: influence of activation methods and pyrolysis temperatures. Environ Geochem Health 37(6):969–983

Parshetti GK, Hoekman SK, Balasubramanian R (2013) Chemical, structural and combustion characteristics of carbonaceous products obtained by hydrothermal carbonization of palm empty fruit bunches. Bioresour Technol 135:683–689

Partovinia A, Rasekh B (2018) Review of the immobilized microbial cell systems for bioremediation of petroleum hydrocarbons polluted environments. Crit Rev Environ Sci Technol 48(1):1–38

Peiris C, Gunatilake SR, Mlsna TE, Mohan D, Vithanage M (2017) Biochar based removal of antibiotic sulfonamides and tetracyclines in aquatic environments: a critical review. Biores Technol 246:150–159

Pereira RC, Kaal J, Arbestain MC, Lorenzo RP, Aitkenhead W, Hedley W, Macías F, Hindmarsh J, Agulló JAM (2011) Contribution to characterisation of biochar to estimate the labile fraction of carbon. Org Geochem 42(11):1331–1342

Pino NJ, Muñera LM, Peñuela GA (2016) Bioaugmentation with Immobilized Microorganisms to Enhance Phytoremediation of PCB-Contaminated Soil. Journal of Soil Contamination 25(4):419–430

Prado A, Berenguer R, Esteve-Núñez A (2019) Electroactive biochar outperforms highly conductive carbon materials for biodegrading pollutants by enhancing microbial extracellular electron transfer. Carbon 146:597–609

Qian LB, Shang X, Zhang B, Zhang WY, Su AQ, Chen Y, Ouyang D, Han L, Yan JC, Chen MF (2018) Enhanced removal of Cr(VI) by silicon rich biochar-supported nanoscale zero-valent iron. Chemosphere 215:739–745

Qiu YP, Zheng ZZ, Zhou ZL, Sheng GD (2009) Effectiveness and mechanisms of dye adsorption on a straw-based biochar. Biores Technol 100(21):5348–5351

Quan GX, Sun WJ, Yan JL, Lan YQ (2014) Nanoscale Zero-Valent Iron Supported on Biochar: Characterization and Reactivity for Degradation of Acid Orange 7 from Aqueous Solution. Water Air Soil Pollut 225(11):1–10

Rafique MI, Usman ARA, Ahmad M, Sallam A, Al-Wabel M (2019) In situ immobilization of Cr and its availability to maize plants in tannery waste–contaminated soil: effects of biochar feedstock and pyrolysis temperature. J Soils Sediments 20:330–339

Rajapaksha AU, Vithanage M, Lim JE, Ahmed MBM, Zhang M, Lee SS, Ok YS (2014) Invasive plant-derived biochar inhibits sulfamethazine uptake by lettuce in soil. Chemosphere 11:500–504

Rajapaksha AU, Alam MS, Chen N, Alessi DS, Igalavithana AD, Tsang DCW, Ok YS (2018) Removal of hexavalent chromium in aqueous solutions using biochar: Chemical and spectroscopic investigations. Sci Total Environ 625:1567–1573

Reza MT, Rottler E, Herklotz L, Wirth B (2015) Hydrothermal carbonization (HTC) of wheat straw: Influence of feedwater pH prepared by acetic acid and potassium hydroxide. Biores Technol 182:336–344

Rinklebe J, Shaheen SM, El-Naggar A, Wang HL, Laing JD, Alessi DS, Ok YS (2020) Redox-induced mobilization of Ag, Sb, Sn, and Tl in the dissolved, colloidal and solid phase of a biochar-treated and un-treated mining soil. Environ Int 140:105754

Ronsse F, Hecke SV, Dickinson D, Prins W (2013) Production and characterization of slow pyrolysis biochar: influence of feedstock type and pyrolysis conditions. Global Chang Biology Bioenergy 5(2):104–115

Rossner A, Snyder SA, Knappe DRU (2009) Removal of emerging contaminants of concern by alternative adsorbents. Water Res 43(15):3787–3796

Schwarzenbach RP, Egli T, Hofstetter TB, Gunten UV, Wehrli B (2010) global water pollution and human health. Soc Sci Electron Publ 35(1):109–136

Sevilla M, Fuerteshe AB (2009) Production of carbon materials by hydrothermal carbonization of cellulose. Carbon 47(9):2281–2289

Sewu DD, Boakye P, Jung H, Woo SH (2017) Synergistic dye adsorption by biochar from co-pyrolysis of spent mushroom substrate and *Saccharina japonica*. Biores Technol 244(1):1142–1149

Shaheen SM, El-Naggar A, Wang JX, Hassan NEE, Niazi NK, Wang HL, Tsang DCW, Ok YS, Bolan N, Rinklebe J (2019) Biochar as an (Im)mobilizing agent for the potentially toxic elements in contaminated soils-science direct. Biochar Biomass Waste 14:255–274

Shakya A, Agarwal T (2019) Removal of Cr(VI) from water using pineapple peel derived biochars: adsorption potential and re-usability assessment. J Mol Liq 93:111497

Shan DN, Deng SB, Zhao TN, Wang B, Wang YJ, Huang J, Yu G, Winglee J, Wiesner MR (2016) Preparation of ultrafne magnetic biochar and activated carbon for pharmaceutical adsorption and subsequent degradation by ball milling. J Hazard Mater 305:156–163

Shang MR, Liu YG, Liu SB, Zeng GM, Tan XF, Jiang LH, Huang XX, Ding Y, Guo YM, Wang SF (2016) A novel graphene oxide coated biochar composite: synthesis, characterization and application for Cr(VI) removal. RSC Adv 88:85202–85212

Shen ZT, Hou DY, Jin F, Shi JX, Fan XL, Tsang DCW, Aless DS (2019) Effect of production temperature on lead removal mechanisms by rice straw biochars. Sci Total Environ 655:751–758

Shinogi Y, Kanri Y (2003) Pyrolysis of plant, animal and human waste: physical and chemical characterization of the pyrolytic products. Biores Technol 90(3):241–247

Sigmund G, Huber D, Bucheli TD, Baumann M, Borth N, Guebitz G, Hofmann T (2017) Cytotoxicity of Biochar: A Workplace Safety Concern? Environ Sci Technol Lett 4(9):362–366

Song ZG, Lian F, Yu ZH, Zhu LY, Xing BS, Qiu WW (2014) Synthesis and characterization of a novel MnOx-loaded biochar and its adsorption properties for Cu^{2+} in aqueous solution. Chem Eng J 242:36–42

Song JY, He QL, Hu XL, Zhang W, Wang CY, Chen RF, Wang HY, Mosa A (2019) Highly efficient removal of Cr(VI) and Cu(II) by biochar derived from *Artemisia argyi* stem. Environ Sci Pollut Res Int 26:13221–13234

Spokas KA, Cantrell KB, Novak JM, Archer DW, Ippolito JA, Collins HP, Boateng AA, Lima IM, Lamb MC, McAloon AJ (2012) Biochar: a synthesis of its agronomic impact beyond carbon sequestration. J Environ Qual 41(4):973–989

Sun YN, Gao B, Yao Y, Fang J, Zhang M, Zhou YM, Chen H, Yang LY (2014) Effects of feedstock type, production method, and pyrolysis temperature on biochar and hydrochar properties. Chem Eng J 120:220–206

Sun JN, He FH, Pan YH, Zhang ZH (2016) Effects of pyrolysis temperature and residence time on physicochemical properties of different biochar types. Acta Agriculturae Scandinavica 67(1):12–22

Taha SM, Amer ME, Elmarsafy AE, Elkady MY (2014) Adsorption of 15 different pesticides on untreated and phosphoric acid treated biochar and charcoal from water. J Environ Chem Eng 2(4):2013–2025

Takaya CA, Fletcher LA, Singh S, Anyikude KU, Ross AB (2016) Phosphate and ammonium sorption capacity of biochar and hydrochar from different wastes. Chemosphere 145:518–527

Tan XF, Liu YG, Zeng GM, Wang X, Hu XJ, Gu YL, Yang ZZ (2015) Application of biochar for the removal of pollutants from aqueous solutions. Chemosphere 125:70–85

Tan GC, Xu N, Xu YR, Wang HY, Sun WL (2016) Sorption of mercury (II) and atrazine by biochar, modified biochars and biochar based activated carbon in aqueous solution. Biores Technol 211:727–735

Tan ZX, Lin CSK, Ji XY, Rainey TJ (2017) Returning biochar to fields: a review. Appl Soil Ecol 116:1–11

Tang JC, Lv HH, Gong YY, Huang Y (2015) Preparation and characterization of a novel graphene/biochar composite for aqueous phenanthrene and mercury removal. Biores Technol 196:355–363

Thang PQ, Jitae K, Giang BL, Viet NM, Huong PT (2019) Potential application of chicken manure biochar towards toxic phenol and 2,4-dinitrophenol in wastewaters. J Environ Manage 251:109556

Thines KR, Abdullah EC, Mubarak NM, Ruthiraan M (2017) Synthesis of magnetic biochar from agricultural waste biomass to enhancing route for waste water and polymer application: a review. Renew Sustain Energy Rev 67:257–276

Uchimiya M, Wartelle LH, Klasson KT, Fortier CA, Lima IM (2011) Influence of pyrolysis temperature on biochar property and function as a heavy metal sorbent in soil. J Agric Food Chem 59(6):2501–2510

Van VN, Zafar M, Behera SK, Park HS (2015) Arsenic(III) removal from aqueous solution by raw and zinc-loaded pine cone biochar: equilibrium, kinetics, and thermodynamics studies. Int J Environ Sci Technol 12(4):1283–1294

Vithanage M, Mayakaduwa SS, Herath I, Ok YS, Mohan D (2015) Kinetics, thermodynamics and mechanistic studies of carbofuran removal using biochars from tea waste and rice husks. Chemosphere 150:781–789

Vo AT, Nguyen VP, Ouakouak A, Nieva A Jr, Tran BTD, Chao HYHP (2019) Efficient removal of Cr(VI) from water by biochar and activated carbon prepared through hydrothermal carbonization and pyrolysis: adsorption-coupled reduction mechanism. Water 11(6):1164

Wahab R, Dwivedi S, Umar A, Singh S, Hwang IH, Shin HS, Musarrat J, Al-Khedhairy AA, Kim YS (2013) ZnO nanoparticles induce oxidative stress in Cloudman S91 melanoma cancer cells. J Biomed Nanotechnol 9:441–449

Wang SZ, Wang JL (2019) Activation of peroxymonosulfate by sludge-derived biochar for the degradation of triclosan in water and wastewater. Chem Eng J 356:350–358

Wang MC, Sheng GD, Qiu YP (2015a) A novel manganese-oxide/biochar composite for efficient removal of lead(II) from aqueous solutions. Int J Environ Sci Technol 12(5):1719–1726

Wang SS, Gao B, Zimmerman AR, Li YC, Harris WG, Migliaccio KW (2015b) Removal of arsenic by magnetic biochar prepared from pinewood and natural hematite. Biores Technol 175:391–395

Wang ZY, Liu GC, Zheng H, Li FM, Ngo HH, Guo WS, Liu C, Chen L, Xing BS (2015c) Investigating the mechanisms of biochar's removal of lead from solution. Biores Technol 177:308–317

Wang YY, Lu HH, Liu YX, Yang SM (2016a) Removal of phosphate from aqueous solution by SiO_2–biochar nanocomposites prepared by pyrolysis of vermiculite treated algal biomass. RSC Adv 6(87):83534–83546

Wang ZQ, Jin PX, Wang M, Wu CH, Dong C, Wu A (2016b) Biomass-derived porous carbonaceous aerogel as sorbent for oil-spill remediation. ACS Appl Mater Interfaces 8(48):32862–32868

Wang J, Liao ZW, Ifthikar J, Shi LR, Chen ZQ, Chen ZL (2017) One-step preparation and application of magnetic sludge-derived biochar on acid orange 7 removal via both adsorption and persulfate based oxidation. RSC Adv 7(30):18696–18706

Wang TF, Zhai YB, Zhu Y, Li CT, Zeng GM (2018) A review of the hydrothermal carbonization of biomass waste for hydrochar formation: Process conditions, fundamentals, and physicochemical properties. Renew Sustain Energy Rev 90:223–247

Wang HY, Chen P, Zhu YG, Chen K, Sun GX (2019a) Simultaneous adsorption and immobilization of As and Cd by birnessite-loaded biochar in water and soil. Environ Sci Pollut Res 26(9):8575–8584

Wang ZP, Liu K, Xie L, Zhu HN, Ji SB, Sun XQ (2019b) Effects of residence time on characteristics of biochars prepared via copyrolysis of sewage sludge and cotton stalks. J Anal Appl Pyrol 142:104659

Wu C, Liu XG, Wu XH, Dong FS, Xu J, Zheng YQ (2019) Sorption, degradation and bioavailability of oxyfluorfen in biochar-amended soils. Sci Total Environ 658:87–94

Xia T, Kovochich M, Brant J, Hotze M, Sempf J, Oberley T, Sioutas C, Yeh JI, Wiesner MR, Nel AE (2006) Comparison of the abilities of ambient and manufactured nanoparticles to induce cellular toxicity according to an oxidative stress paradigm. Nano Lett 6(8):1794–1807

Xie T, Reddy KR, Wang CW, Yargicoglu E, Spokas K (2015) Characteristics and applications of biochar for environmental remediation: a review. Crit Rev Environ Sci Technol 45(9):939–969

Xu XY, Schierz A, Xu N, Cao XD (2016) Comparison of the characteristics and mechanisms of Hg(II) sorption by biochars and activated carbon. J Colloid Interface Sci 463:55–60

Xu CB, Zhao JW, Yang WJ, Wei WX, Tan X, Wang J, Lin AJ (2020) Evaluation of biochar pyrolyzed from kitchen waste, corn straw, and peanut hulls on immobilization of Pb and Cd in contaminated soil. Environ Pollut 261:114133

Xue YW, Gao B, Yao Y, Inyang M, Zhang M, Zimmerman AR, Ro KS (2012) Hydrogen peroxide modification enhances the ability of biochar (hydrochar) produced from hydrothermal carbonization of peanut hull to remove aqueous heavy metals: Batch and column tests. Chem Eng J 200–202:673–680

Yan LL, Kong L, Qu Z, Li L, Shen GQ (2015) Magnetic biochar decorated with ZnS nanocrytals for Pb (II) removal. ACS Sustain Chem Eng 3(1):125–132

Yang X, Zhang SQ, Ju MT, Liu L (2019) Preparation and modification of biochar materials and their application in soil remediation. Appl Sci 9(7):1365

Yao L, Yang H, Chen ZS, Qiu MQ, Hu BW, Wang XX (2020) Bismuth oxychloride-based materials for the removal of organic pollutants in wastewater. Chemosphere. https://doi.org/10.1016/j.chemosphere.2020.128576

Yi SZ, Sun YY, Hu X, Xu HX, Gao B, Wu JC (2017) Porous nano-cerium oxide wood chip biochar composites for aqueous levofloxacin removal and sorption mechanism insights. Environ Sci Pollut Res 25(26):25629–25637

Yue Y, Shen CC, Ge Y (2019) Biochar accelerates the removal of tetracyclines and their intermediates by altering soil properties. J Hazard Mater 380:120821

Zeng ZT, Ye SJ, Wu HP, Xiao R, Zeng GM, Liang J, Zhang C, Yu JF, Fang YL, Song B (2019) Research on the sustainable efficacy of g-MoS_2 decorated biochar nanocomposites for removing tetracycline hydrochloride from antibiotic-polluted aqueous solution. Sci Total Environ 648:206–217

Zhang M, Gao B (2013) Removal of arsenic, methylene blue, and phosphate by biochar/AlOOH nanocomposite. Chem Eng J 226:286–292

Zhang P, Sun HW, Yu L, Sun TH (2013) Adsorption and catalytic hydrolysis of carbaryl and atrazine on pig manure-derived biochars: Impact of structural properties of biochars. J Hazard Mater 244–245:217–224

Zhang MM, Liu YG, Li TT, Xu WH, Zheng BH, Tan XF, Wang H, Guo YM, Guo FY, Wang SF (2015) Chitosan modification of magnetic biochar produced from Eichhornia crassipes for enhanced sorption of Cr(VI) from aqueous solution. RSC Adv 5(58):46955–46964

Zhang MY, Song LH, Jiang HF, Li S, Shao YF, Yang JQ, Li JF (2017a) Biomass based hydrogel as an adsorbent for the fast removal of heavy metal ions from aqueous solutions. J Mater Chem A 5(7):3434–3446

Zhang XP, Li YS, Li H (2017b) Enhanced Bio-Immobilization of Pb Contaminated Soil by Immobilized Bacteria with Biochar as Carrier. Pol J Environ Stud 26(1):413–418

Zhang DJ, Li Y, Tong SQ, Jiang XB, Wang LJ, Sun XY, Li JS, Liu XD, Shen JY (2018) Biochar supported sulfide-modified nanoscale zero-valent iron for the reduction of nitrobenzene. RSC Adv 8(39):22161–22168

Zhang LK, Guo JY, Huang XM, Wamg WD, Sun P, Li YM, Han JH (2019a) Functionalized biochar-supported magnetic MnFe$_2$O$_4$ nanocomposite for the removal of Pb(II) and Cd(II). RSC Adv 9:365–376

Zhang LK, Mao JF, Chen BL (2019b) Reconsideration of heterostructures of biochars: morphology, particle size, elemental position, reactivity and toxicity. Environ Pollut 254:113017

Zhang QM, Saleem M, Wang CX (2019c) Effects of biochar on the earthworm (Eisenia foetida) in soil contaminated with and/or without pesticide mesotrione. Sci Total Environ 671:52–58

Zhang H, Xiao R, Li RH, Ali A, Chen A, Zhang ZQ (2020a) Enhanced aqueous Cr(VI) removal using chitosan-modified magnetic biochars derived from bamboo residues. Chemosphere 261:127694

Zhang Y, Zhao GM, Xuan Y, Gan L, Pan MZ (2020b) Enhanced photocatalytic performance for phenol degradation using ZnO modified with nano-biochar derived from cellulose nanocrystals. Cellulose 28:991–1009

Zhao B, O'Connor D, Zhang JL, Peng TY, Shen ZT, Tsang DCW, Hou D (2018) Effect of pyrolysis temperature, heating rate, and residence time on rapeseed stem derived biochar. J Clean Prod 174:977–987

Zheng W, Guo MX, Chow T, Bennett DN, Rajagopalan N (2010) Sorption properties of greenwaste biochar for two triazine pesticides. J Hazard Mater 181(1–3):121–126

Zheng H, Liu BJ, Liu GC, Cai ZH, Zhang CC (2019) Potential toxic compounds in biochar: knowledge gaps between biochar research and safety: biochar from biomass and waste. Fund Appl 19:349–384

Zhou JL, Zhang ZL, Banks E, Grover D, Jiang JQ (2009) Pharmaceutical residues in wastewater treatment works effluents and their impact on receiving river water. J Hazard Mater 166(2–3):655–661

Zhou L, Liu YG, Liu SB, Yin YC, Zeng GM, Tan XF, Hu X, Hu XJ, Jiang LH, Ding Y, Liu SH, Huang XX (2016) Investigation of the adsorption-reduction mechanisms of hexavalent chromium by ramie biochars of different pyrolytic temperatures. Biores Technol 218:351–359

Zhou QW, Liao BH, Lin LN, Qiu WW, Song ZG (2018) Adsorption of Cu(II) and Cd(II) from aqueous solutions by ferromanganese binary oxide-biochar composites. Sci Total Environ 615:115–122

Zhu DQ, Pignatello JJ (2005) Characterization of aromatic compound sorptive interactions with black carbon (Charcoal) assisted by graphite as a model. Environ Sci Technol 39(7):2033–2041

Zhu Y, Yi BJ, Yuan QX, Wu YL, Wang M (2018a) Removal of methylene blue from aqueous solution by cattle manure-derived low temperature biochar. RSC Adv 8(36):19917–19929

Zhu YL, Zheng C, Wu SY, Song ZY, Hu BW (2018b) Interaction of Eu(III) on magnetic biochar investigated by batch, spectroscopic and modeling techniques. J Radioanal Nucl Chem 316(3):1337–1346